

Article

The Effect of Internal Combustion Engine Nozzle Needle Profile on Fuel Atomization Quality

Oleh Klyus ¹, Marcin Szczepanek ^{2,*} , Grzegorz Kidacki ³, Paweł Krause ³, Sławomir Olszowski ⁴ and Leszek Chybowski ^{5,*} 

¹ Department of Marine Power Plants, Faculty of Marine Engineering, Maritime University of Szczecin, ul. Willowa 2, 71-650 Szczecin, Poland; o.klyus@pm.szczecin.pl

² Department of Power Engineering, Faculty of Marine Engineering, Maritime University of Szczecin, ul. Willowa 2, 71-650 Szczecin, Poland

³ Faculty Teaching Centre, Faculty of Marine Engineering, Maritime University of Szczecin, ul. Willowa 2, 71-650 Szczecin, Poland; g.kidacki@gmail.com (G.K.); pawelkrause20@gmail.com (P.K.)

⁴ Department of Operation and Transport Organization, Faculty of Transport and Electrical Engineering, Kazimierz Pułaski University of Technology and Humanities in Radom, ul. Malczewskiego 29, 26-600 Radom, Poland; s.olszowski@uthrad.pl

⁵ Department of Machine Construction and Materials, Faculty of Marine Engineering, Maritime University of Szczecin, ul. Willowa 2, 71-650 Szczecin, Poland

* Correspondence: m.szczepanek@pm.szczecin.pl (M.S.); l.chybowski@pm.szczecin.pl (L.C.); Tel.: +48-91-48-09-376 (M.S.); +48-91-48-09-412 (L.C.)

Abstract: This article presents the results of research on the impact of changing the cross-section of an atomizer's flow channel, which is caused by changing the flow geometry of the passive part of the needle on the drop diameter distribution of the fuel spray. A three-hole type H1LMK, 148/1 atomizer with hole diameters, d_N , equal to 0.34 mm, is analyzed. A nozzle with a standard (i.e., unmodified) needle and three nozzles using needles with a modified profile in the flow part of the needle, marked by the code signatures 1L, 2L, and 3L, are tested. An increasing level of fuel turbulence characterizes the needles during the flow along their flow part due to the use of one (1L), two (2L), and three (3L) de Laval toroidal nozzles, respectively, obtained by mechanically shaping the outer surface of the flow part of the spray needle. The spray produced is tested using the Malvern Spraytec STP 500 device cooperating with the dedicated Malvern version 4.0. During the tests, measurements and an analysis of the spray droplet size distribution over the entire injection duration, equal to 7 ± 2 ms, are made for each nozzle. The experiment makes it possible to determine the effect of the nozzle needles' profiles on the time distribution of the actual droplet diameters; the time distribution of the Sauter mean droplet diameters, $D_{[3,2]}$; the percentile shares of the droplet diameters $D_v(10)$, $D_v(50)$, and $D_v(90)$; the distribution span during the development of the spray stream; and the time distribution of the shares of the droplets with diameters belonging to selected diameter classes $D_{[x1-x2]}$ in the spray. The results of the measurements of the drop diameter distribution indicate that using atomizers with a modification to the flow channel allows for an increase in the share of droplets with smaller diameters compared to the standard atomizer.

Keywords: fuel nozzle; modified needle; fuel injection; atomization quality; droplet distribution



Citation: Klyus, O.; Szczepanek, M.; Kidacki, G.; Krause, P.; Olszowski, S.; Chybowski, L. The Effect of Internal Combustion Engine Nozzle Needle Profile on Fuel Atomization Quality. *Energies* **2024**, *17*, 266. <https://doi.org/10.3390/en17010266>

Academic Editor: Christopher Micallef

Received: 6 December 2023

Revised: 31 December 2023

Accepted: 2 January 2024

Published: 4 January 2024



Copyright: © 2024 by the authors. Licensee MDPI, Basel, Switzerland. This article is an open access article distributed under the terms and conditions of the Creative Commons Attribution (CC BY) license (<https://creativecommons.org/licenses/by/4.0/>).

1. Introduction

1.1. Modification of the Characteristics of a Combustible Mixture

The correct operation of an internal combustion engine, in the context of its reliability and the minimization of the specific fuel consumption and emission of toxic compounds via exhaust gases, is possible, among others, by creating a combustible mixture with the appropriate characteristics. This possibly applies to the homogeneous atomization of the fuel in the entire volume of the combustion chamber, proper fragmentation of the

fuel dose fed into the cylinder, and even mixing of fuel and air in the entire combustible mixture. The listed characteristics of the combustible mixture are usually obtained by appropriately shaping the air intake duct (the spiral-shaped inlet and swirling blades) [1,2], the combustion chamber [3] (the shape of the piston crown and the shape of the surface of the cylinder head closing the combustion chamber) [4,5], the proper atomization of the fuel by the injector [6,7], additional devices and ignition delay [8], and fuel injection strategy [9].

In diesel engines, fuel is injected into the combustion chamber at the end of the compression stroke. From the moment the injection (which raises the injector needle) starts to the moment the fuel ignited (for which an increase in the pressure in the combustion chamber is noticeable), the period of time referred to as ignition delay elapses. During this period, the sprayed dose of fuel absorbs heat from the air compressed in the combustion chamber, and the fuel evaporates and ignites spontaneously (i.e., local ignition centers form). The fuel flowing into the combustion chamber is still ignited and burned by the flame propagating in the combustion chamber.

The ignition delay determines the course of the combustion (parameters) and the loads on the elements of the crank–piston system [10] and [11] (pp. 30–48), the thermal efficiency [12,13], the intake air parameters [14], and the emissions of harmful exhaust components [12,15].

Ignition delay is described using various numerical indices, including a cetane number (CN) and equivalent indices deriving from the cetane number, diesel index, and calculated ignition index [16–18]. A higher CN value corresponds to fuels with a shorter ignition delay [19]. The ignition delay depends on the fuel's properties, such as the specific heat capacity, vapor pressure, heat of boiling and diffusivity, and degree of fragmentation of the stream (drop diameters) [20–22].

1.2. Fuel Droplet Size Distribution

As indicated above, after being injected via the injector into the combustion chamber, the fuel evaporates and mixes with air [23]. These are the factors that are necessary to create a homogeneous combustible mixture [24]. The time in which the fuel evaporates is approximately 0.05 to 0.005 s [25]. In order for the fuel evaporation process to run effectively, it is necessary to atomize the fuel properly. The Sauter mean diameter (i.e., the volume–area average droplet diameter, $D_{[3,2]}$) is used to determine the atomization quality [26,27] (also referred to as *SMD*), which expresses the ratio of the volume to the surface area of a drop, in real and equivalent streams, for this diameter [28,29]. After being injected into the combustion chamber, the fuel stream breaks into millions of droplets with Sauter mean diameters of 5–10 μm [25] (pp. 35–41) in high-speed engines and 15–25 μm in low-speed engines [25] (pp. 35–41) and [30].

According to the ISO 9276-2 standard and the moment–ratio notation, the general definition of mean particle size is described using the following formula [31]:

$$\bar{D}_{[p,q]} = \left(\frac{\sum_{i=1}^N n_i D_i^p}{\sum_{i=1}^N n_i D_i^q} \right)^{\frac{1}{p-q}}, \quad (1)$$

where D represents the particle diameter, i is the number of particles in a size class with an upper particle size of x_i , n is the number of particles in the i -th class, and N is the number of size classes.

The Sauter mean diameter, $D_{[3,2]}$, is defined as the mean particle size in terms of the volume diameter, $D_{[3,0]}$, and the surface diameter, $D_{[2,0]}$, of the particle. The following relationship describes the Sauter diameter [26,27]:

$$D_{[3,2]} = \frac{D_{[3,0]}^3}{D_{[2,0]}^2} = \frac{6V_p}{A_p}, \quad (2)$$

where A_p signifies the external particle surface area, and V_p is the particle volume.

For a single molecule, the following dependencies arise:

$$D_{[3.0]} = \sqrt[3]{\frac{6V_p}{\pi}}, \quad (3)$$

$$D_{[2.0]} = \sqrt{\frac{A_p}{\pi}}. \quad (4)$$

The average Sauter diameter is, thus, determined according to the following formula:

$$\bar{D}_{[3,2]} = \frac{(\overline{D_{[3.0]}})^3}{(\overline{D_{[2.0]}})^2} = \frac{\sum_{i=1}^N n_i D_i^3}{\sum_{i=1}^N n_i D_i^2}. \quad (5)$$

Note that the average diameter of the droplets does not provide information about the largest droplets. In the full spectrum of stream droplet diameters, there are drops with sizes close to the maximum, and they basically determine the shape of the designed combustion chamber, as their presence affects the extension of the stream range. Therefore, to assess the suitability of a given injector for a specific combustion chamber, the information related to the volume fraction of the droplets of various sizes, D_v , and the width of the SPAN droplet diameter distribution is important.

The following values of $D_v < 10\% v/v$, $D_v < 50\% v/v$, and $D_v < 90\% v/v$ are droplet size percentile distributions by volume, which indicate the maximum droplet size falling within 10%, 50%, or 90% of the droplet sizes of the total mixture volume [7], and $D_v < 10\% v/v$, $D_v < 50\% v/v$, and $D_v < 90\% v/v$ in the simplified notation in the following part of the article are marked as $D_v(10)$, $D_v(50)$, and $D_v(90)$, respectively [32]. The span of the statistical distribution of droplet sizes in the mixture volume is determined using the following relationship [33]:

$$SPAN = \frac{D_V(< 90\% v/v) - D_V(< 10\% v/v)}{D_V(< 50\% v/v)} = \frac{D_V(90) - D_V(10)}{D_V(50)}. \quad (6)$$

The literature on the subject provides many test results of injectors and nozzles for diesel engines with direct injection. The nature of the fuel stream disintegration depends mainly on the following factors [25]:

- Fuel flow rate from the nozzle;
- Density of the fuel and the density of the medium into which the fuel is injected;
- Fuel intermolecular bonds (fuel viscosity and surface tension);
- Effects of the aerodynamic drag forces of the medium into which the fuel is injected;
- Dimensions and shape of the discharge channel.

The stream of the atomized fuel should have a shape that correlates with the shape of the combustion chamber, ensuring intensive mixing with air. This enables the formation of a combustible mixture of an appropriate quality [34]. Fuel droplets with diameters that allow for evaporation at the pressure and temperature of the air compressed in the chamber absorb heat from the environment and turn it into gas, mixing with the air. Self-ignition of the fuel–air mixture occurs when the following conditions are met simultaneously: the mixture of fuel and air is stoichiometric (in practice, an appropriate excess air factor, λ , is ensured) and is of the appropriate pressure and temperature.

The proper disintegration of the “tree” occurs because of the influence of aerodynamic forces, whose share in the formation of droplets increases with the speed of fuel flow from the atomizer nozzle. These forces create resistance to the fuel penetrating the medium into which it is injected, which results in the stream breaking into drops at a certain distance from the fuel outlet of the atomizer nozzle [35,36]. The medium into which the fuel is injected is air mixed with exhaust gas residues from the previous working cycle or, in the

case of parts of dual-fuel gas engines, this medium is a mixture of gaseous fuel and air together with exhaust gas residues.

Aerodynamic drag forces depend on the fuel flow velocity, the density of the medium into which the fuel is injected, and the front surface of the stream. For outflow velocities greater than 80 m/s, fuel stream disintegration is usually observed at the very outflow from the atomizer nozzle. Depending on the type of engine (injector), it is assumed that the fuel flow rate should be 250–400 m/s [25], although other sources indicate lower values of 100–200 m/s [37].

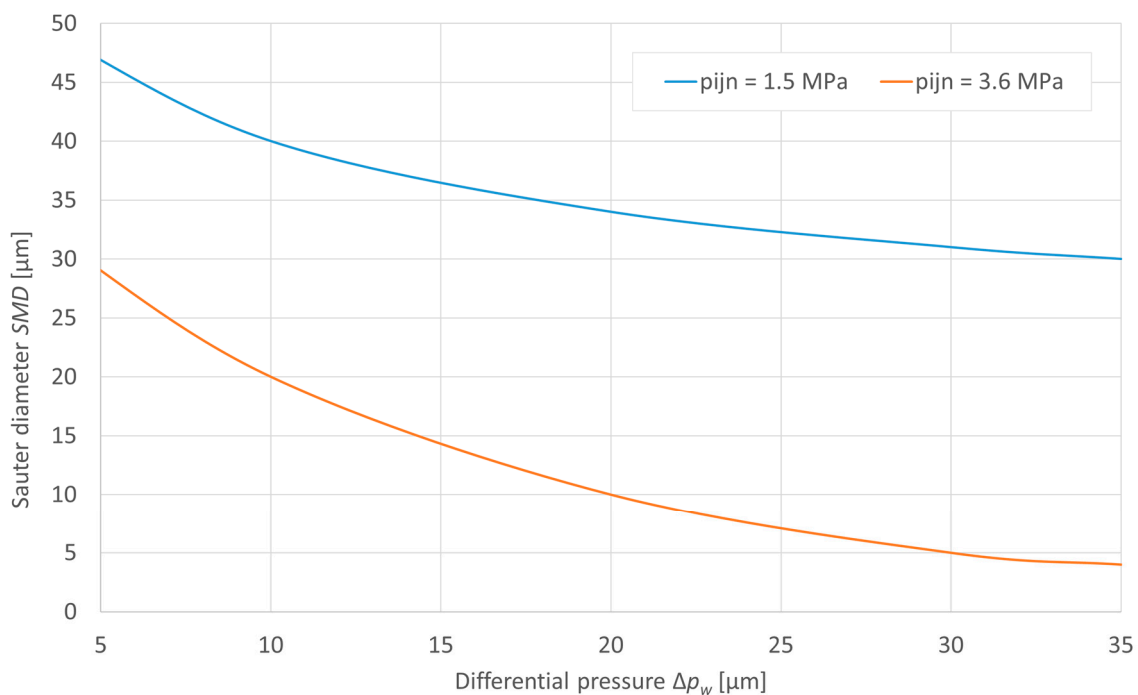
Ensuring the appropriate speed is achieved by selecting a sufficiently high fuel injection pressure, which nowadays reaches maximum values in the range of up to 300 mPa and, in the case of marine engines, these values reach approximately 100 mPa. The injector opening pressures are set in accordance with the engine manufacturer's guidelines and, in the case of marine engines, are usually 23–45 mPa.

The fuel flow rate (in units of m/s) from the atomizer nozzle can be described using the transformed Bernoulli equation in the following form:

$$w = \varphi \sqrt{\frac{2 \cdot \Delta p_w}{\rho}} = \varphi \sqrt{\frac{2(p_{inj} - p_{air})}{\rho}}. \quad (7)$$

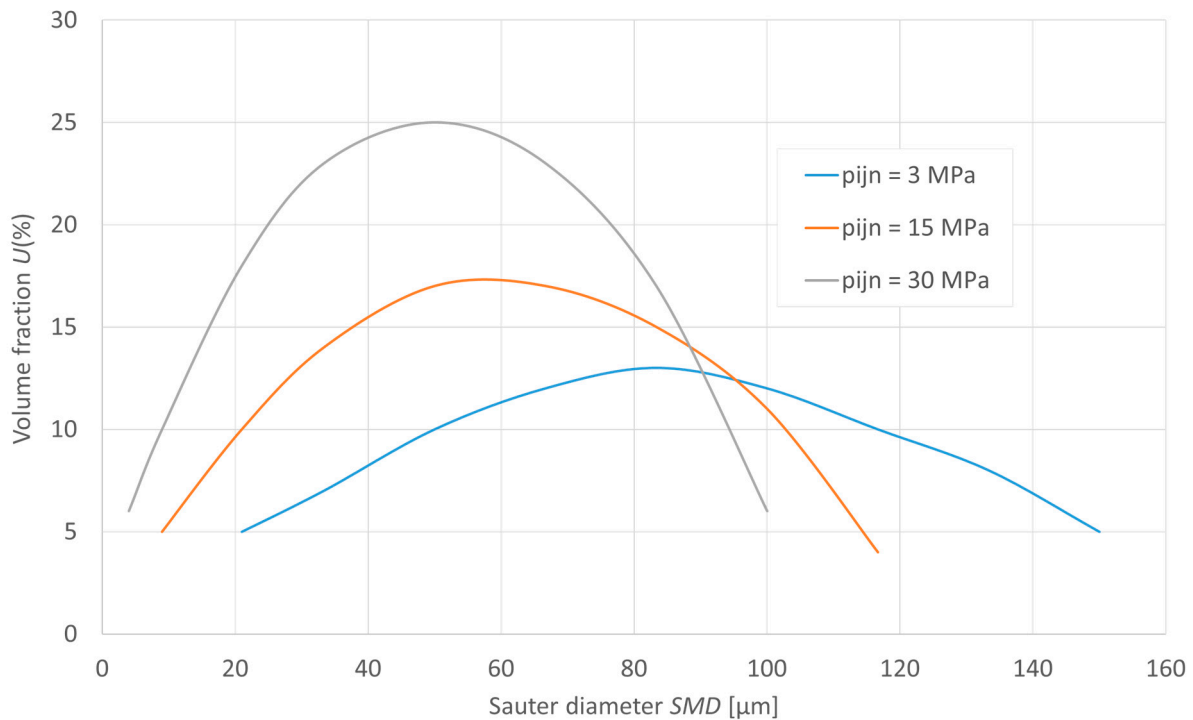
where Δp_w denotes the differential pressure (in units of Pa), p_{inj} is the injection pressure (Pa), p_{air} is the air pressure in the space to which the fuel injection is performed (Pa), ρ is the density of the injected fuel (kg/m^3), and φ is the discharge coefficient including losses related to the shape of the atomizer nozzle's channel (which usually assumes values in the range of 0.65–0.90).

The effect of changing the injection pressure and the pressure of the medium into which the fuel is injected on the change in the size of the aerosol droplets is shown in Figure 1.



(a)

Figure 1. Cont.



(b)

Figure 1. Influence of the injection pressure and air pressure on the aerosol droplet size (based on Ref. [25]): (a) Sauter mean diameter (SMD); (b) volume fraction. p_{inj} —Injection pressure.

The quality of the fuel atomization is also affected by its viscosity, which is a measure of the friction forces inside the fluid [38,39]. Viscosity, thus, directly affects the spray angle, fuel jet penetration, and droplet size [40–42]. For marine engines running on residual fuels, the fuel is heated so that the viscosity of the fuel before the injector meets the engine manufacturer’s requirements, typically 10–20 mm²/s (10–20 cSt) [43]. In the case of distillate fuels, the fuel viscosities are <10 mm²/s (<10 cSt), which is due to the composition of these fuels [44].

1.3. Criterion Numbers Characterizing Fuel Flow

Hiroyasu et al. [45] developed empirical relationships between the kinematic viscosity, ν (m²/s); density, ρ (kg/m³); nozzle diameter, d_N (mm); and Sauter mean diameter, $D_{[3,2]}$, in a sprayed aerosol. For complete atomization, the formula has the following form [45]:

$$D_{[3,2]} \approx d_N Re^{0.25} We^{-0.32} \left(\frac{\mu}{\mu_a} \right)^{0.37} \left(\frac{\rho}{\rho_a} \right)^{-0.47} \approx d_N \nu^{0.12} \rho^{-0.42}. \quad (8)$$

where Re signifies the Reynolds number of the fuel jet, We is the Weber number of the fuel jet, μ is the dynamic viscosity of the fuel (Pa·s), μ_a is the dynamic viscosity of the air (medium) (Pa·s), and ρ_a is the density of the air (medium) (kg/m³).

The Weber number, We , is a dimensionless criterion number measuring the relative importance of the fluid’s inertia (disruptive aerodynamic forces) compared to the surface tension cohesive forces, σ (N/m). The We number is described using the following formula:

$$We = \frac{\rho w^2 d_N}{\sigma}. \quad (9)$$

The Reynolds number, Re , is a dimensionless criterion number, which is a measure of the ratio between the inertial and viscous forces. The Re number is described using the following expression:

$$Re = \frac{wd_N}{\nu} = \frac{\rho wd_N}{\mu}. \quad (10)$$

where ρ (kg/m^3) denotes the fuel density (kg/m^3), w is the discharge velocity (m/s), d_N is the characteristic linear dimension (nozzle diameter) (mm), ν is the kinematic viscosity of the fluid (m^2/s), and μ is the dynamic viscosity of the fluid ($\text{Pa}\cdot\text{s}$).

The Reynolds number, Re , is used as a criterion for flow turbulence. Turbulent flow occurs when the critical value for Re is exceeded. It is different for different cross-sections and flow conditions. In the case of a typical nozzle duct for compression–ignition engines, the criteria for the circular cross-section of the duct can be adopted. However, the ratio of the duct length of the atomizer nozzle to the duct diameter, d_N (L/D_N ratio), of typical ducts is significantly below 10 [46,47], for which the flow will not stabilize. In addition, the injection dynamics and engine vibrations may cause the phenomenon to occur at much lower Re values compared to its results from theoretical calculations. Therefore, the value of Re cannot be relied upon solely as a criterion for the turbulence of the flow in an atomizer channel of a compression ignition engine.

Ohnesorge showed that for the same values of dynamic viscosity, density, surface tension (physical properties of the fuel), and constant diameter of the nozzle orifice, as the outflow velocity increases, the liquid streams undergo different mechanisms of primary disintegration, starting from a droplet, through transient, turbulent, and proper disintegration [48]. As the speed increases, the size of the droplets becomes smaller. Ohnesorge graphically presented the experimental results using a criterion number which, as a function of the Reynolds number, Re , determines the areas of the stream decay mechanisms. The Ohnesorge number, Oh , is a dimensionless number that relates the viscous forces to inertial and surface tension forces according to the following relationship:

$$Oh = \frac{\sqrt{We}}{Re} = \frac{\mu}{\sqrt{\rho\sigma d_n}}. \quad (11)$$

On the basis of research by other scientists in later years, the stream decay model was modified [49]. However, the qualitative description of the phenomenon described by Ohnesorge was confirmed [46]. Further analysis of the phenomena in the atomizer channel led most researchers to the conclusion that the fragmentation of the stream flowing from the atomizer is determined by the phenomena occurring in the atomizer channel (nozzle) [50]. One of the most important factors determining the decay mechanism of the primary stream flowing out of the hole is turbulence [46,47], as well as the accompanying cavitation [51,52] and abrasive wear [44,53]. The phenomenon of cavitation is beneficial for the creation of an appropriate jet of injected fuel [54] but also causes wear of the injectors (i.e., cavitation erosion in the injectors), which is the subject of separate studies [55].

Cavitation bubbles (liquid vapor bubbles, in this case, fuel) are caused by low static pressure appearing behind the sharp edges of the nozzle channel inlet [56]. At high flow rates, the liquid tends to detach from the channel walls, forming a vena contracta [51]. The constriction reduces the cross-sectional area of the fluid flow, increasing fluid flow velocity and static pressure drop around the constriction. Vena contracta causes narrowing of the effective cross-section of the liquid stream, which affects the reduction in the fuel mass stream \dot{m} (kg/s). This relation is captured by the discharge coefficient C_D [57,58]:

$$C_D = \frac{\dot{m}}{\rho w A}, \quad (12)$$

where A is the area at the nozzle's exit (m^2).

The pressure in the flowing fuel may drop below the vapor pressure of the liquid at a given temperature, and bubbles of liquid vapor may appear that are lifted into the stream and rapidly disappear (imploding) in its higher-pressure areas [59]. Implosions can also destabilize the liquid stream and its atomization, resulting in the shortening of the liquid core and the range of the stream due to improved fragmentation [60].

The dimensionless cavitation number, K , is used as a quantitative criterion for classifying the intensity of the cavitation phenomenon in nozzle holes [50,61]. The K parameter is directly proportional to the injection pressure difference and the vapor pressure and inversely proportional to the injection pressure difference and the outlet cross-section of the nozzle opening. An increase in the number of Re causes a decrease in the parameter K . Mohan et al. [62] found that cavitation flow occurs when the K number drops below 1.7. At the same time, they observed a decrease in the value of the CD index to 0.85–0.81.

Park et al. [63] showed the influence of the presence of cavitation in the flow through nozzle holes on the quality of the atomization measured, $D_{[3,2]}$. Diesel oil and biofuel were used for the experiment. The mean droplet diameter was determined for turbulent and cavitation flows. The experiment showed a relatively slight decrease in the $D_{[3,2]}$ value for both diesel oil and biofuel. It should be noted that the tests were carried out using single-hole nozzles with a hole diameter of $d_N = 6$ mm (2 lengths, $L/d_N = 1.5$, and $L/d_N = 3$) and injection pressures up to 0.45 MPa. At the same time, these studies showed the influence of the geometry of the nozzle opening (L/d_N) on the flow type. A longer channel required a higher pressure (about 25%) to obtain the cavitation phenomenon.

Moreover, the shape of the atomizer nozzle's channels affects the type of flow, which was studied for elliptical cross-sections of atomizer holes by Molina et al. [64]. In addition, the surface condition of the atomizer nozzle's channels is an important factor in increasing the turbulence of the flowing fuel. Winklhofer et al. [65] showed the influence of the increase in the roughness of the inner surface of the channels in an atomizer nozzle on the faster occurrence of the cavitation phenomenon in the flowing fuel.

1.4. Motivation for the Experimental Research Performed

As can be seen from the above review of the literature, researchers on the subject analyzed various issues related to the formation of the jet and the intensification of its disintegration while considering the properties of the fuel and the characteristics of the outflow channels from the atomizer nozzle (i.e., shape, surface condition, and dimensions). He et al. obtained several research results on the influence of injector nozzle's geometry on turbulence in flowing fuel [66,67]. Research was also conducted on the intensification of the fuel turbulence inside the nozzle [68]. In the available literature, however, there are few research results on the influence of the shape of the free (passive) part of the needle (i.e., the section between the cone and the guiding element) on the structure of a sprayed fuel stream.

Klyus et al. [69], using simulation tests for a needle with helical intersecting grooves on its free surface, showed an increase in turbulence in the channels of the nozzle holes in relation to a needle with a smooth cylindrical surface. The research was related to developing modified fuel injectors characterized by increased turbulence in the atomizer nozzle [70] and using a de Laval nozzle [71].

The present research displays the further development of these studies by the experimental determination of the nozzle needle's profile's effect on the generated spray's characteristics. This article also presents the results of testing an injector for diesel engines with a spray nozzle, whose free part of the needle has a variable cross-section and, together with the housing, forms a fuel flow channel with a variable cross-section.

This study examined the effect of changing the geometry of the needle's free part on the fuel stream's atomization quality. As quality criteria, the value of the Sauter mean diameter, $D_{[3,2]}$ (i.e., the volumetric distributions of the numbers of droplets belonging to specific size classes and constituting specific volume shares in the entire volume of the generated spray), and the width of the *SPAN* droplet size distribution were adopted. Hence,

this paper intends to confirm the previous simulations in an experimental manner. The research question answered in this paper is whether the results of the measurements of the drop diameter distribution indicate that using atomizers with modified flow channels allows for an increase in the share of droplets with smaller diameters compared to a standard atomizer.

2. Materials and Methods

This research aimed to compare the effects of three changes to the cross-section of a nozzle's flow channels caused by a change in the flow geometry of the passive part of the needle on the drop diameter distribution of the fuel spray that forms during injection into the medium under atmospheric pressure. A comparison of the three selected modifications to the needle's shape with a standard solution for a typical injector commonly used in fishing fleet engines was performed. In this experiment, we determined the effect of the nozzle needle's profile on the following:

- Distribution of the actual droplet diameters depending on the spray stream's development time interval;
- Time distribution of the Sauter mean diameter, $D_{[3,2]}$, depending on the spray stream's development time interval;
- Percentiles of the droplet diameters $D_v(10)$, $D_v(50)$, and $D_v(90)$, representing, respectively, 10%, 50%, and 90% of the volume of the generated spray;
- Distribution span of the percentiles of the SPAN droplet diameters during the development of the spray stream;
- Time distribution of the selected diameter classes, $D_{[x1-x2]}$, during the development of the spray stream.

The W1F-01 fuel injector used in the research presented in this article had a three-hole nozzle H1LMK 148/1 (PZL-WZM, Jawczyce, Poland), with hole diameters of $d_N = 0.34$ mm and an atomizer channel length of $L = 1.2$ mm. A nozzle with a standard (unmodified) needle, marked by the symbol "S", and three nozzles with needles that have a modified profile in the flow part of the needle, marked by the code signatures 1L, 2L, and 3L, were tested (Figure 2). The length of the passive part of the needle with the conical section was equal to 24.5 mm. The diameter of the passive part of the S needle was equal to 5 mm.

Modification of the channels of the flow part (passive) was used to increase the turbulence of the fuel when flowing through the nozzle's outlet channel. An increasing level of fuel turbulence characterized the nozzle needles during the flow along their flow part due to the use of one (1L), two (2L), and three (3L) de Laval toroidal nozzles, respectively, obtained by mechanically shaping the outer surface of the flow part of the spray needle. The injectors were adjusted to the standard nozzle opening pressure of 26 mPa, and the fuel stream was introduced into the air at atmospheric pressure. The temperature of the fuel in front of the injector and the temperature of the medium dispersing the jet (air) was 20 °C. The fuel injector was installed on a test bench and powered using a fuel pump.

The tests were carried out at the stand shown in Figure 3. The station consisted of a manipulation chamber of a laboratory fume cupboard (1), with the exhaust of the vapors by means of mechanical ventilation (2), ending with a stream absorber (3), using gravitational discharge of the liquid to the fuel leakage tank (4) to reduce the risk associated with the presence of fuel spray and vapors. The injector (5) was mounted onto a stand (6) equipped with the ability to make precise adjustments to the stream discharge angle and the distance of the atomizer from the laser measuring axis. Only one stream was observed, while the others were discharged through the deflectors (7) to the fuel leakage tank. As a result, an undisturbed image of the effects of spraying a single stream was obtained, and the influence of ambient parameters on the results of the optical background measurement was reduced. The fuel pressure was generated utilizing a manual device for testing injectors, type PRW 2M (WSK, Krakow, Poland) (8), with a maximum working pressure of 35 Mpa [72], equipped with a fuel tank (9), a fuel filter (10), a plunger pump (11), and a pressure gauge (12).

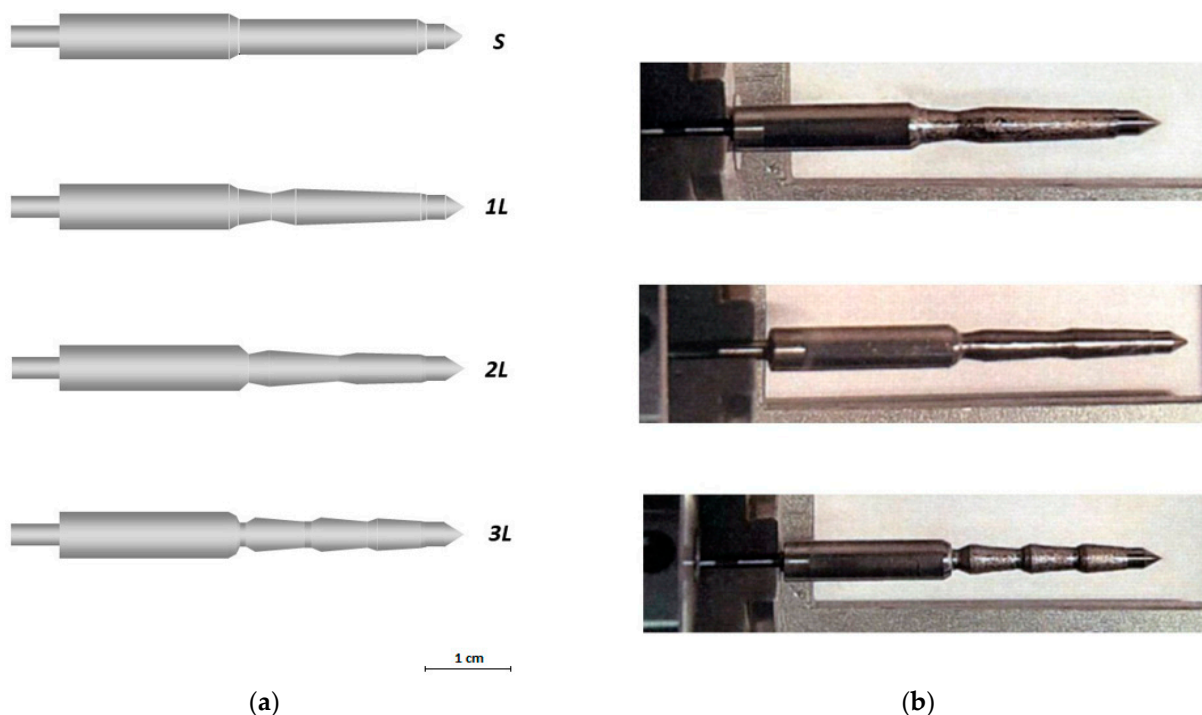


Figure 2. H1LMK 148/1 nozzle needles: (a) profiles used in the tests; (b) photographs of an example.

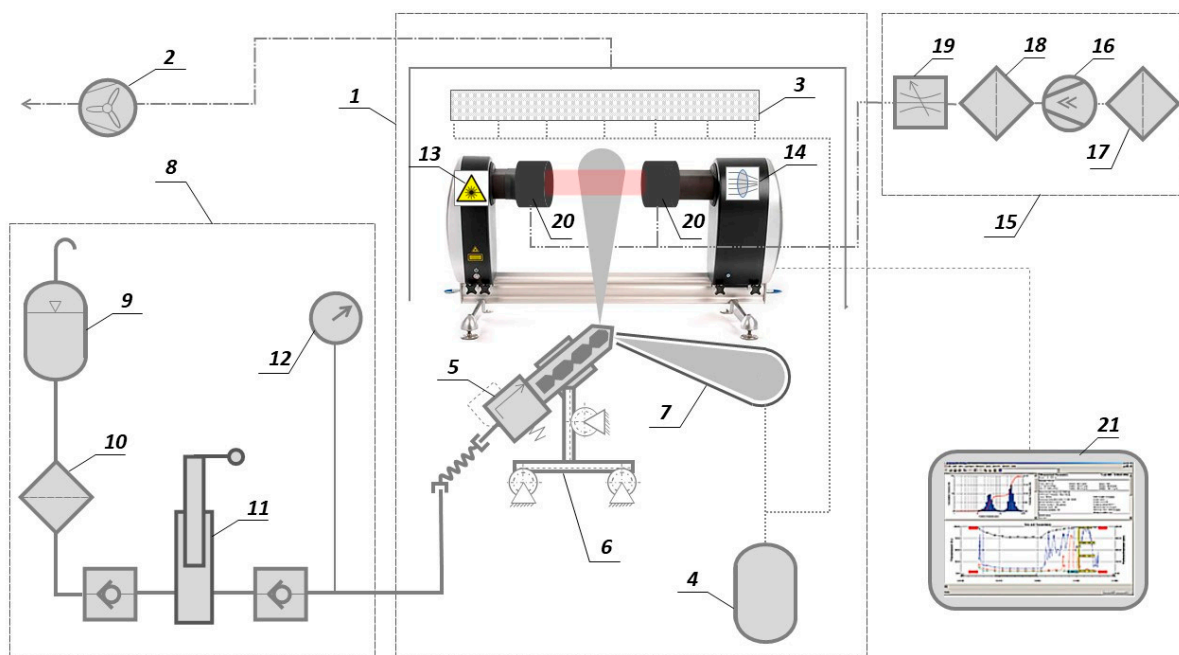


Figure 3. Measuring stand (description in the text).

The analysis of the drop diameter distribution of the fuel droplets was carried out using a Malvern Spraytec STP 500 device (Malvern Instruments, Worcestershire, United Kingdom) [33], designed to measure the diameter of the particles in the sprays based on laser diffraction using the optical model of the Mie theory [73] and Fraunhofer approximations [74].

When calibrated using the NIST standard latex spray, the accuracy, repeatability of the results, and reproducibility among similar devices were greater than $\pm 1\%$ for a diameter of D_v (50). Thanks to the multiple scattering correction system, the device allows for measurements at high spray concentrations, and the maximum sampling frequency was

1 kHz. During the tests, diesel oil without biocomponents (D100) was used as the test fuel. The basic properties of the fuel used in the experiment are listed in Table 1.

Table 1. D100 fuel characteristics.

No.	Parameter	Value	Unit
1.	Density at 15 °C	828.5	kg/m ³
2.	Kinematic viscosity at 40 °C	2.456	mm ² /s
3.	Cetane number	54	-
4.	Flashpoint (determined in a close cup)	60.5	°C
5.	Cold filter plugging point temperature	−29	°C
6.	Cloud point	−8	°C
7.	Water content	0.003%	m/m
8.	Coking residue (10% distillation residue)	0.09%	m/m
9.	Impurity content	8	mg/kg
10.	Lubricity, wear scar diameter WSD1.4 at 60 °C	343	µm
11.	Corrosive action on copper plates	1a	-
12.	Lower calorific value	42.73	MJ/kg

All measurements of the drop diameter distribution of the droplets of both types of fuel were made at a constant distance of the horizontal laser beam from the nozzle outlet, equal to 80 mm, in accordance with Figure 4. This resulted from the need to properly match the spray generation and the measurement systems and was the result of the authors' previous experience [6,7,69]. The fuel jet was horizontal and intersected the laser beam at right angles.

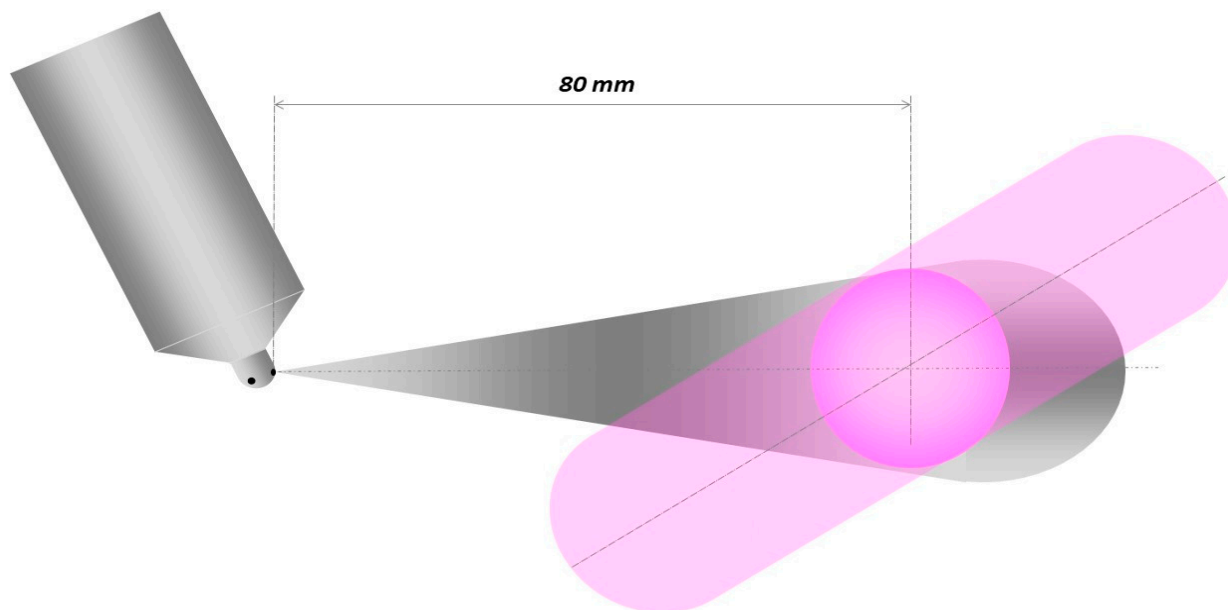


Figure 4. Measurement of the aerosol droplet diameter distribution.

The same preset volumetric fuel dose of 0.6 cm³ was delivered during each injection, set with the pump stroke adjustment screw. The experiment was repeated six times for each type of atomizer using the same fuel, with the standard sampling frequency of the optical system equal to 1 kHz. Statistically derived parameters were calculated based on the arithmetic means of all measurements in the series.

Finite element method (FEM) model studies have shown that modifying the flow channel increases the fuel turbulence's intensity and kinetic energy [26]. The research presented in the article was intended to provide an answer to the question of whether the intensity of the flow turbulence in a modified atomizer channel significantly affects the drop diameter distribution of the fuel, which is part of broader research relating to the

optimization of the design of the injection system of a typical diesel engine used in fishing fleets. The necessity of such tests results from the limited possibilities of changing the operating parameters of these engines, including the angles characterizing the timing of the fuel pumps, inlet valves, and exhaust valves, as well as the injector opening pressure. Changing these parameters directly affects the combustion process's efficiency and engine exhaust gas emissions [26].

The results of the measurements of the fuel spray diameter distribution, produced using a standard atomizer with a flow channel that has a constant cross-section, were compared with the results obtained for the three versions of the atomizer with a channel with a variable cross-section resulting from the use of single (1L), double (2L), or triple (3L) de Laval nozzles.

The atomization quality criterion used for the analysis of the results was, as previously mentioned, determined in experiments: the percentage distribution of the spray diameter ranges; the Sauter mean diameter, $D_{[3,2]}$; the spread of the droplet distribution calculated on the basis of the percentile diameters $D_v(10)$, $D_v(50)$, and $D_v(90)$; and the percentage of droplets with diameters falling within the diameter ranges (i.e., diameter classes) $D_{[1-20]}$, $D_{[20-40]}$, $D_{[40-100]}$, and $D_{[100-1000]}$ (the numbers in indexes are diameter ranges in micrometers for a given diameter class). The classes were selected considering the ranges relevant to the course of the combustion process; typically, these are analyzed in the scientific literature.

3. Results and Discussion

3.1. Temporal Percentage Distribution of Aerosol Fuel Droplet Diameters

The time distribution of aerosol droplet development after fuel injection is shown in the form of 3D graphs in Figures 5–8. The obtained results indicate that regardless of the stream development phase, there was a characteristic maximum in the range of 5–100 μm for each type of nozzle needle. However, it was clearly dependent on the construction of the nozzle. During fuel injection, the width of the diameter range changed alongside the maximum value (in the range of an 8–25% share).

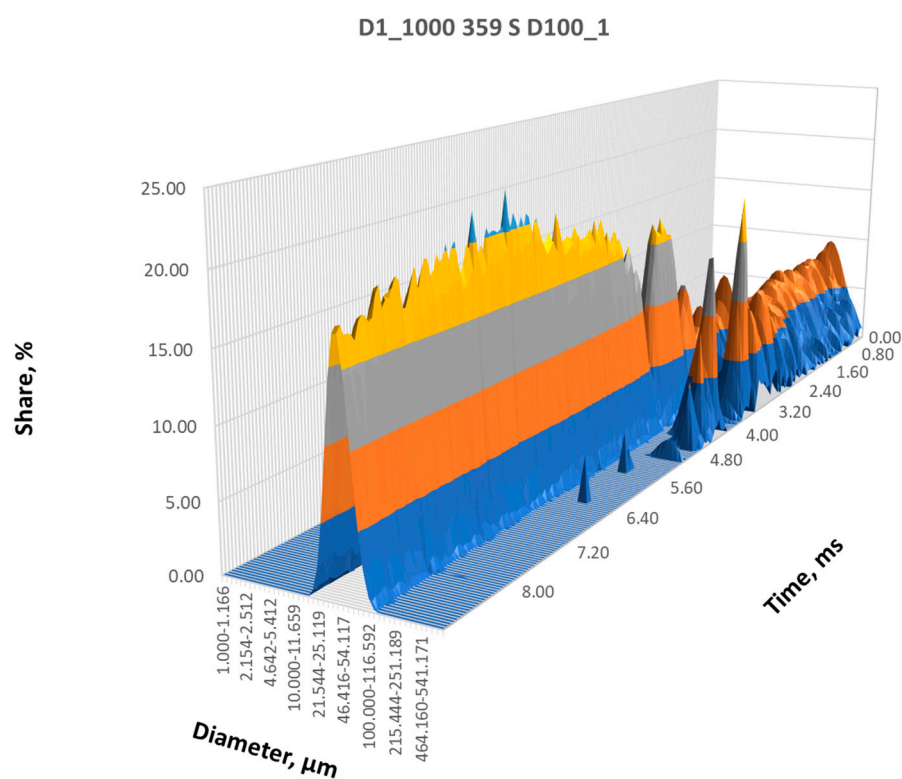


Figure 5. Time distribution of the fuel droplet diameter ranges during the atomization process using an atomizer with a standard (unmodified) needle.

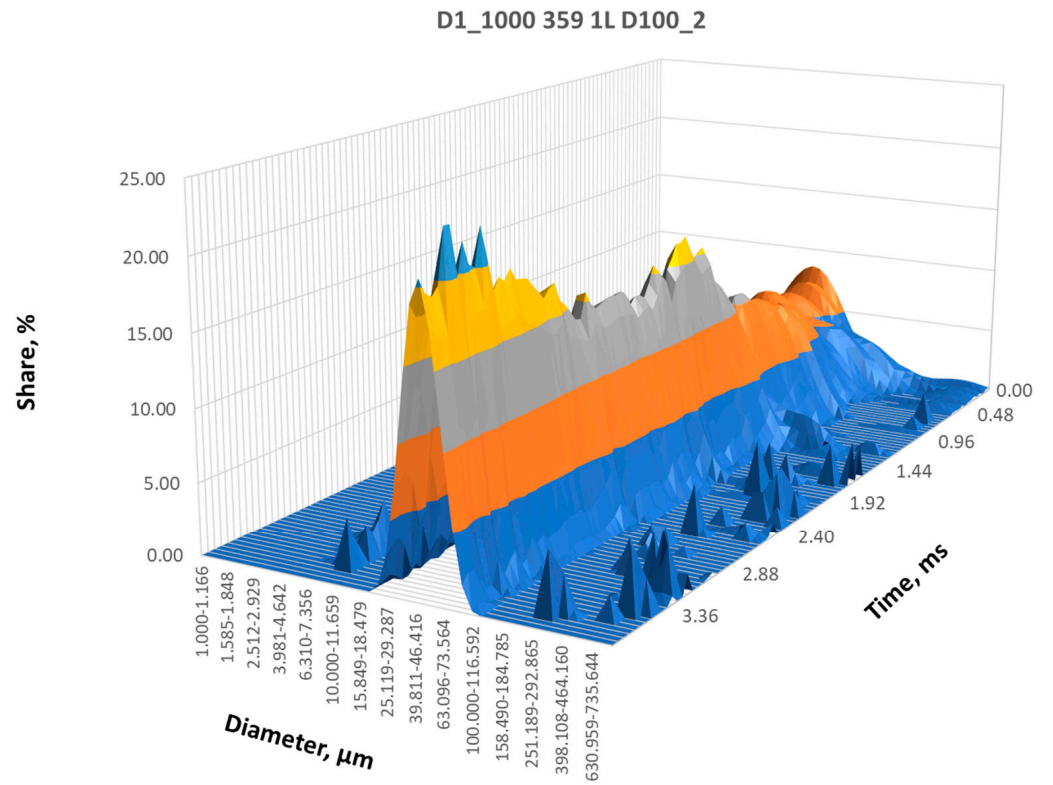


Figure 6. Time distribution of the fuel droplet diameter intervals during the spraying process using a nozzle with a needle profile containing one de Laval nozzle (1L).

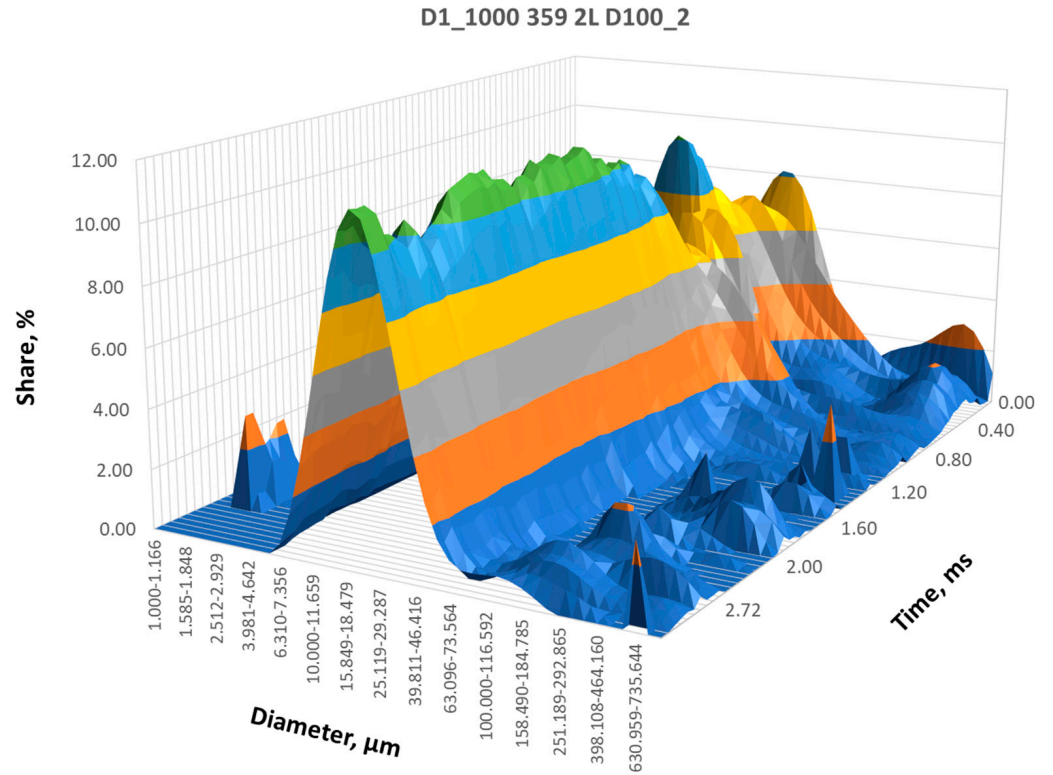


Figure 7. Time distribution of the fuel droplet diameter ranges during the spraying process using a nozzle with a needle profile containing two de Laval nozzles (2L).

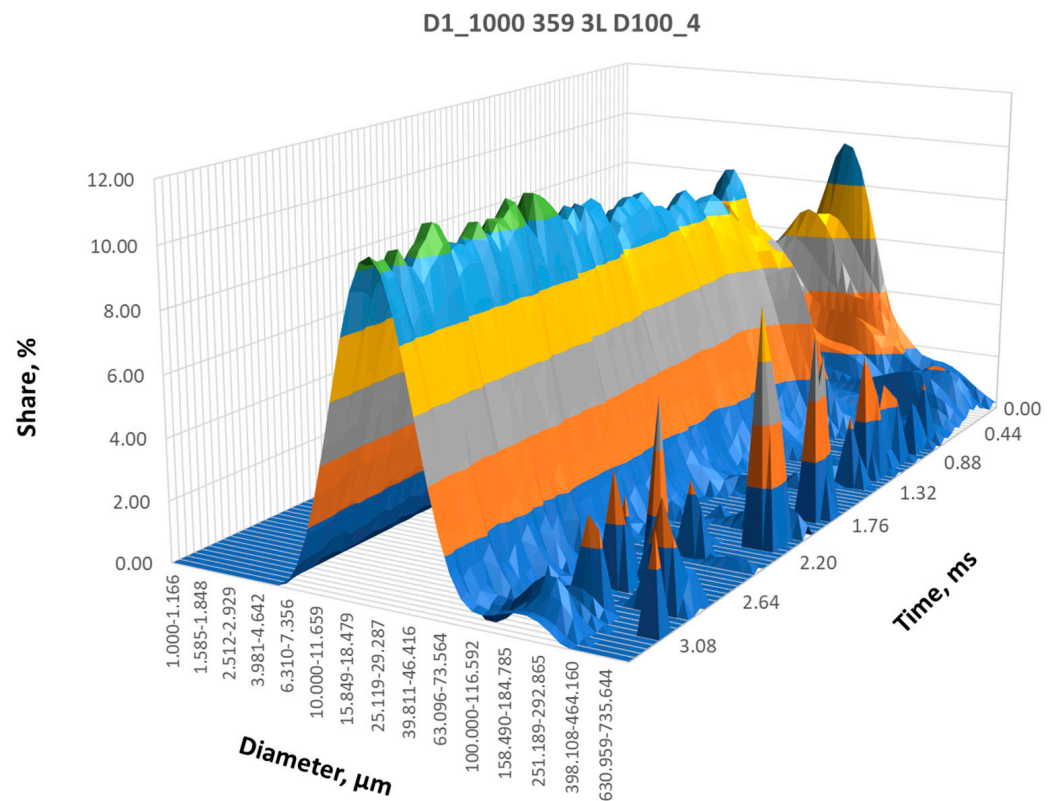


Figure 8. Time distribution of the fuel droplet diameter intervals during the spraying process using a nozzle with a needle profile containing three de Laval nozzles (3L).

In the initial phase of stream development, when the stream density was at its highest, there was less variation in the percentages of the diameters. The maximum line reached the extreme in the standard nozzle (Figure 5) near the middle of the jet's development time interval and modified nozzles only in the second half and at the end of the injection process (Figures 6–8).

The maximum area in the second half of the time interval in the standard nozzle corresponded to the range of diameters from 69 to 73 μm , and in the modified nozzles from 34 to 63 μm , respectively, for the 1L needle (Figure 6); from 11 to 40 μm for the 2L needle (Figure 7); and, similarly, from 14 to 40 μm for the 3L needle (Figure 8).

The total jet development time differed despite an identical volumetric dose of fuel for all versions of the atomizer (Figure 9). This is due to the temporary optical characteristics of the fuel aerosol stream. Measurements were performed using an automatic triggering of the start and end of particle size analysis. The parameter triggering the analyzer's operation is the recorded level of laser light transmission (relating to the transparency of the medium). The change in the transmission over time for different versions of the atomizer proves the level of extinction of the laser beam and the related instantaneous optical density of the medium. A comparison of the laser beam transmission time distributions, obtained as a result of experiments using a standard atomizer and its modifications, shows that the light transmission through the aerosol during the tests was similar and, in all cases, for 2 ms after the start of the injection, it exceeded 70%; after 3 ms, it exceeded 85%.

At the same time, during the initial phase of atomization, clear differences in the time distribution of the light transmission were observed, indicating a different nature of the fuel stream's development in the standard atomizer compared to the modified atomizers. The transmission of the light beam through the aerosol for the standard atomizer showed a minimum during the time interval of approximately 2 ms after the start of the measurement. In contrast, for the modified atomizers, the transmission minimum was observed much earlier, approximately 0.25 ms after the start of the measurement. Despite the identical

thickness of the aerosol layer resulting from the method of conducting the measurements, the level of the minimum transmission of the laser beam was six times lower for the 2L and 3L atomizers compared to the standard solution.

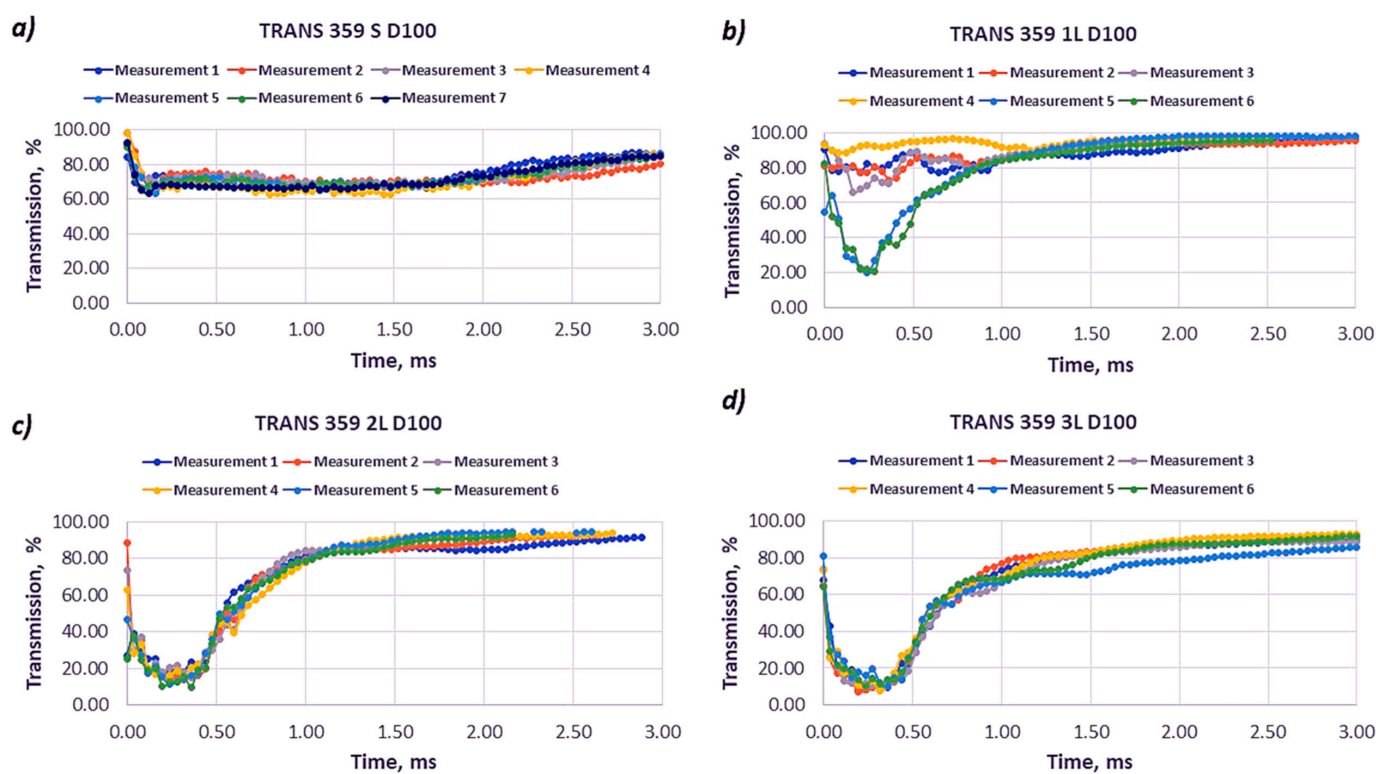


Figure 9. Time distribution of light transmission in the initial phase of the injection for different nozzle versions: (a) with a standard needle; with a needle profile containing (b) one de Laval nozzle, (c) two de Laval nozzles, and (d) three de Laval nozzles.

The 1L atomizer showed too high of a transmission fluctuation in the analyzed time interval to assess the atomization's effects. The transmission results indicate much higher absorption and scattering of the laser beam by aerosols produced in the modified atomizers, occurring just after the start of the measurement.

A high extinction coefficient indicates a higher number of smaller particles, which was confirmed by further analysis of the experimental results. At the same time, there was a significant difference in the length of the time intervals, after which the transmission reached a high level of 90%. For the standard nozzle, it was about 4 ms, while with the modified nozzles, the same level of transmission was achieved in the twice as short amount of a time of the order of 2 ms. This suggests a much shorter course of aerosol formation with smaller droplet diameters during the injection of the same volumetric dose of fuel in the modified nozzles compared to the standard nozzle.

An important supplement to the 3D diameter time distribution charts is the total percentage share of the specified aerosol diameter ranges for the entire injection time in each measurement series, as shown in Figures 10–13.

Particle size distributions provide information on the degree of atomization, which is, apart from uniformity, the basic measure of atomization quality. Regardless of the type of atomizer (figures in associated dataset), the distribution diagrams are bimodal, characterized by the presence of the two most numerous diameter ranges, which differ significantly in absolute value. Between them, a minimum percentage corresponds to a diameter of about 150 μm .

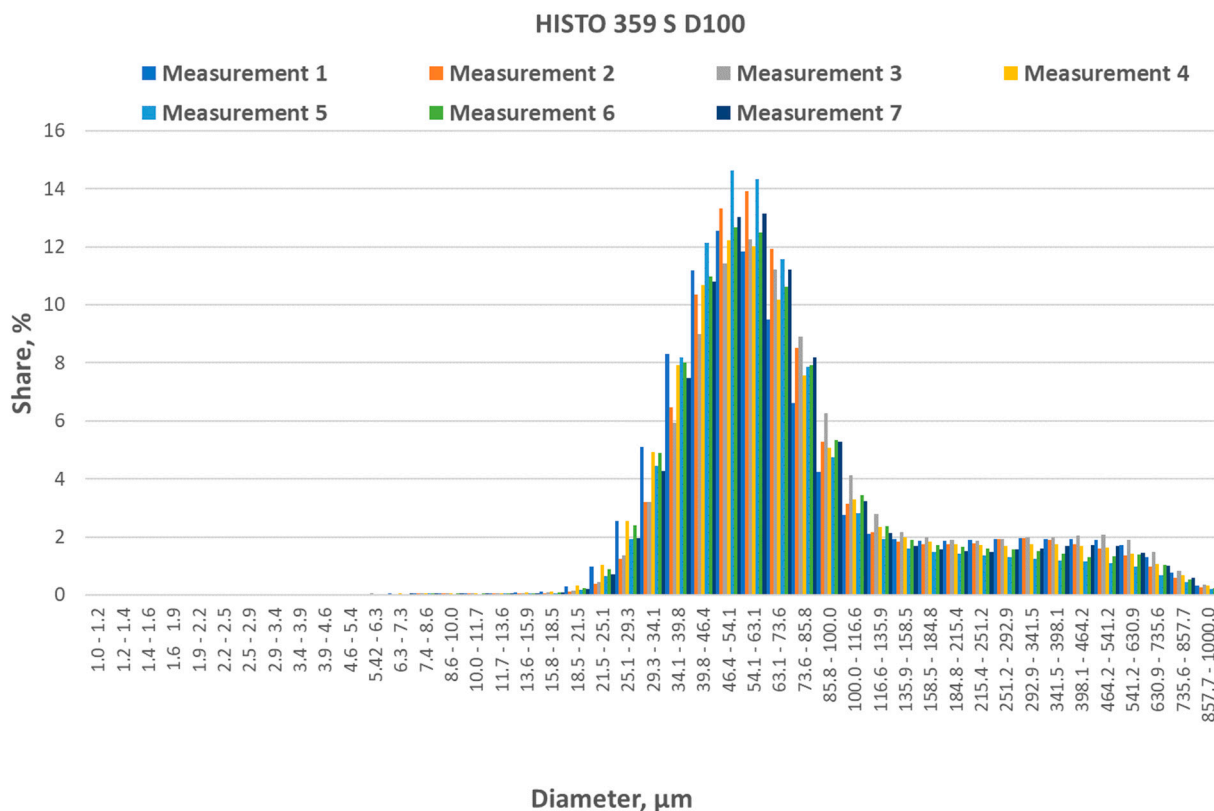


Figure 10. Particle size distribution of the fuel aerosol in successive moments obtained for the atomizer with a standard (i.e., unmodified) needle.

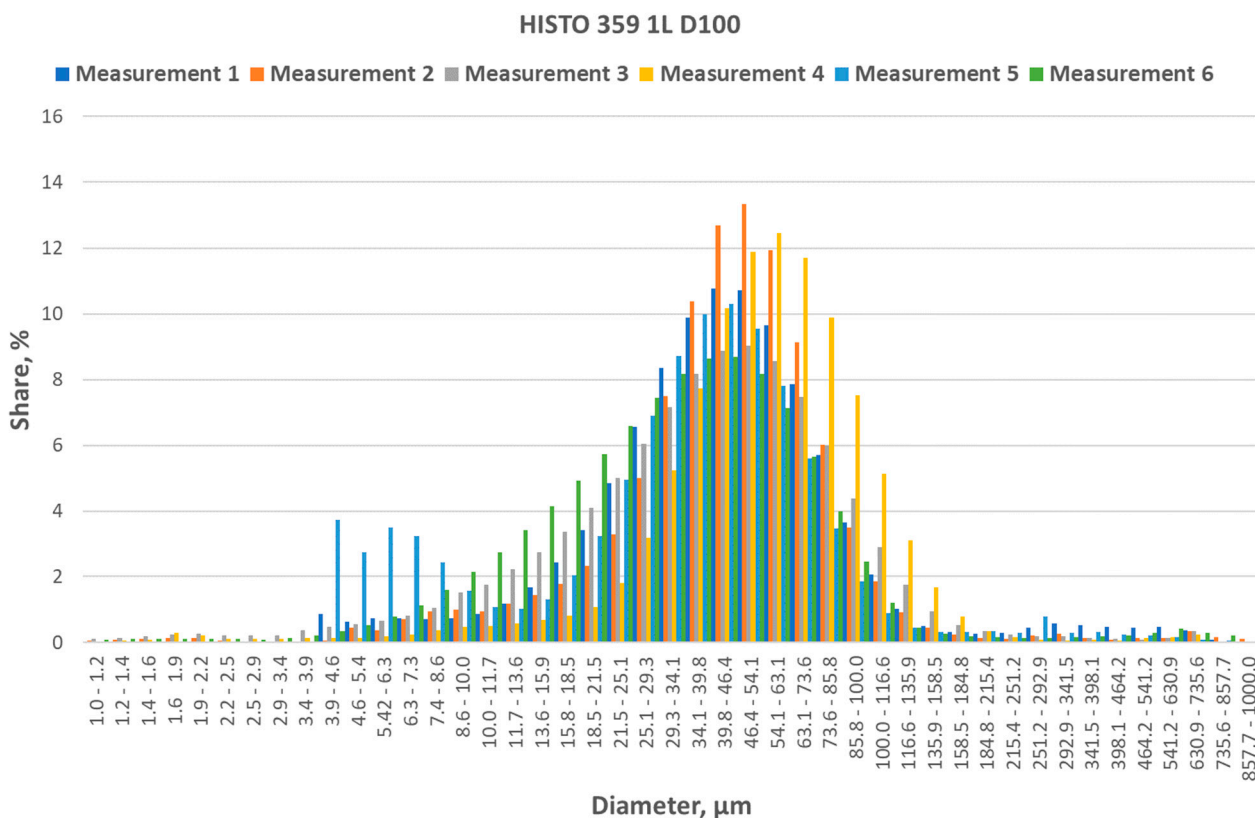


Figure 11. Particle size distribution of the fuel aerosol in successive moments obtained for the sprayer with a needle profile containing one de Laval nozzle (1L).

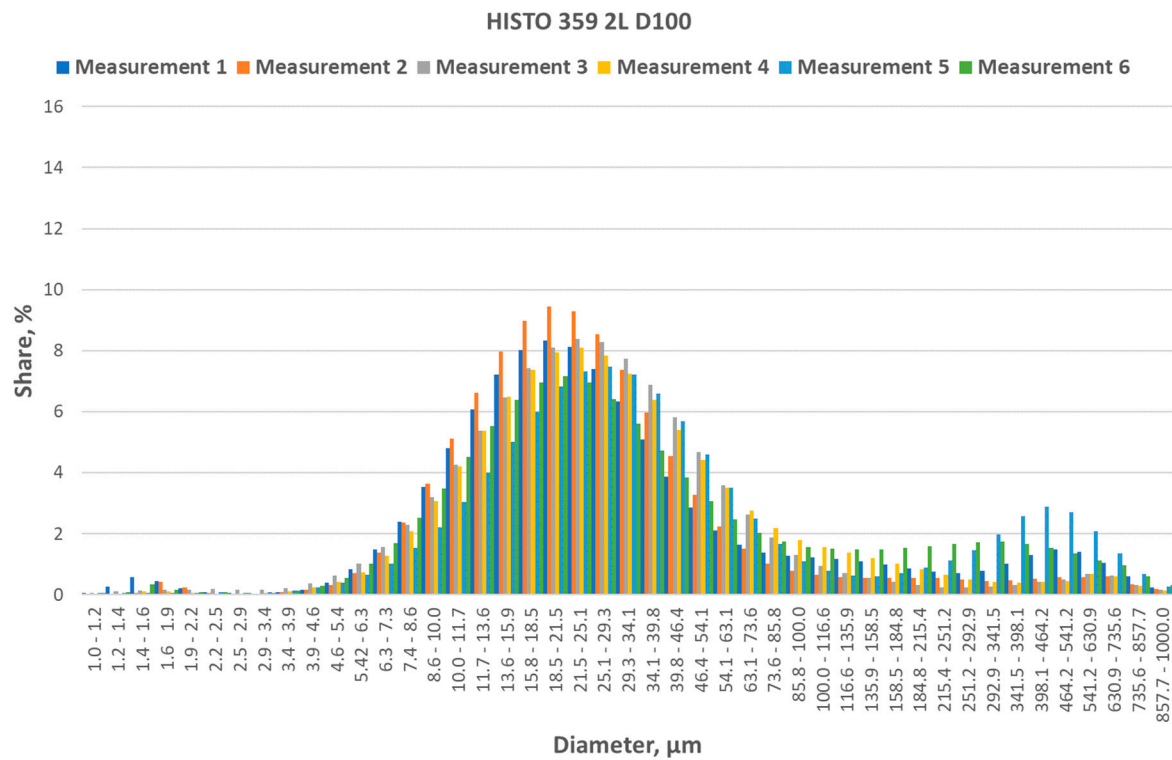


Figure 12. Particle size distribution of the fuel aerosol in successive moments obtained for the atomizer with a needle profile containing two de Laval nozzles (2L).

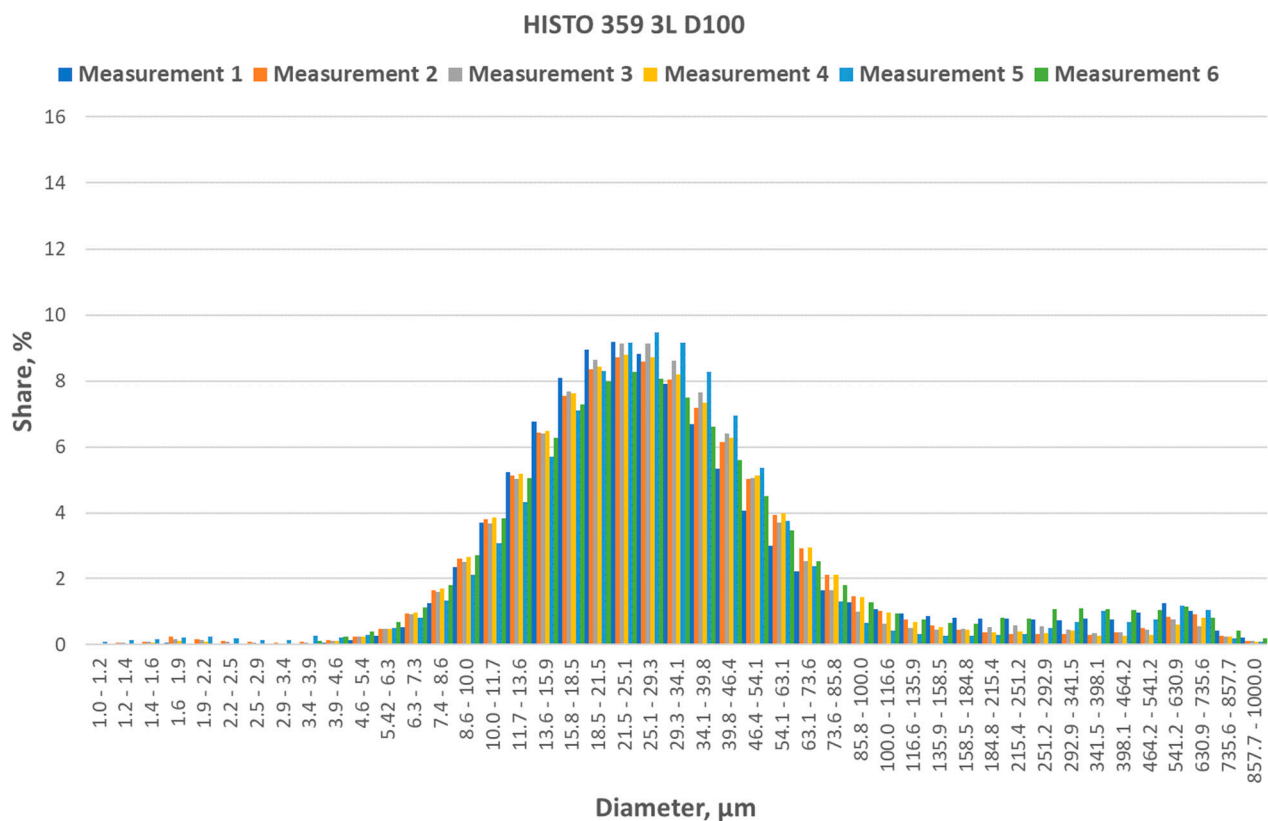


Figure 13. Particle size distribution of the fuel aerosol in successive moments obtained for the atomizer with a needle profile containing three de Laval nozzles (3L).

The presence of the first main modal value below 150 μm resulted from the intended use of the atomizer and is an expected phenomenon. Its absolute value and position relative to the abscissa axis is an important measure of the degree of atomization. It proves the average parameters of the spray in the entire volume of the stream. The presence of the second, lower modal value, located above 150 μm , is the result of the presence of the stream core, in which the degree of atomization was lower due to the weaker interaction of the friction of the dispersing medium and the more intense interaction of the spray droplets. A comparison of the average values of the spray droplet diameter distribution for various atomizers is shown in Figure 14. This figure contains combined data of the measurements from individual cycles. The research data are provided in the dataset attached with the article [75].

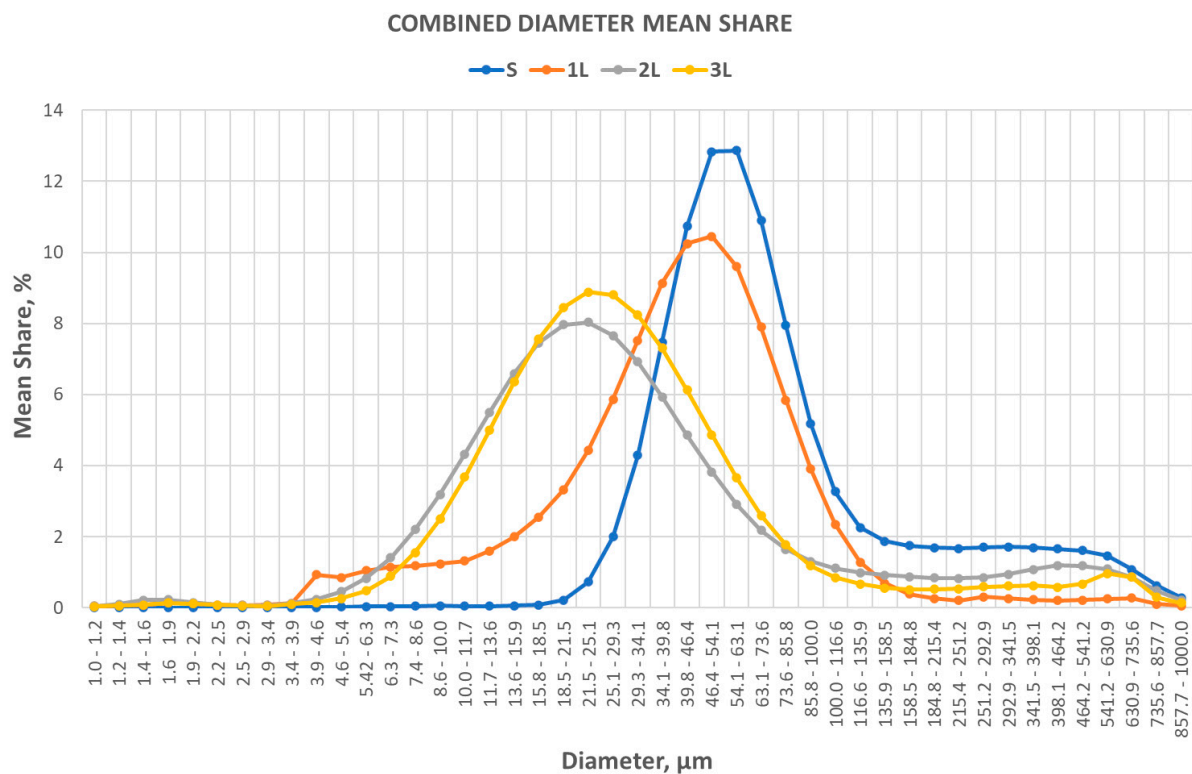


Figure 14. Average values of the drop diameter distribution of the fuel droplets for different spray needle versions.

The main modal value of the standard nozzle was in the diameter range of 54.1–63.1 μm , and its average for all series of measurements was 12.87%. The width of the interval two-thirds around the modal value covers the diameter range from 29.2 to 100.0 μm . With the increase in the number of nozzles in the atomizer's flow channel, the distribution's main modal value shifts toward smaller diameters and decreases its absolute value. Simultaneously, the width of the interval two-thirds around the modal value increases. For the 1L nozzle, the average modal value decreases to 10.45% and is in the diameter range of 46.4–54.1 μm , and the two-thirds range covers the range from 21.5 to 85.7 μm . In the 2L and 3L nozzles, the modal values are in the same diameter range of 21.5–25.1 μm , and their absolute levels are 8.0% and 8.9%, respectively. The width of the two-thirds intervals around the modal value covers diameter ranges of 8.6–54.1 μm for the 2L nozzle and 10.0–54.1 μm for the 3L nozzle.

The second modal value of the diameter distribution is subject to much smaller changes. The standard nozzle is in the range of 292.9–341.4 μm , with the highest value equal to 1.72% of the share in the volume distribution of the diameters. It follows that that modification of the needle results in widening the distribution and lowering the modal

value of the particle diameter distribution. The 1L nozzle is characterized by having the lowest average absolute value of 0.31%, with a simultaneous shift in the occurrence range toward lower averages of 251.2–292.9 μm . In the remaining nozzles, the average modal value is 1.19% of the volume distribution of the diameters for 2L and 0.96% for 3L, with the area of occurrence shifting to larger diameters, respectively, 398.1–464.2 μm for the 2L nozzle and 541.2–631.0 μm for 3L.

The results of the measurement of the drop diameter distribution indicate that the use of nozzles with a modification of the flow channel allows for an increase in the share of drops with smaller diameters compared to the standard nozzle. This is due to the greater degree of atomization, which is one of the two conditions for improving atomization quality. Shifting the distribution of the droplet diameters toward smaller values is vital from the point of view of the fuel injection and combustion process in a compression–ignition engine. A spray dominated by drops with diameters in the range of 20–40 μm provides the shortest ignition delay and combustion time. Drops with smaller diameters have lower kinetic energy, which is insufficient for the proper penetration of the combustion chamber and ensures an adequate macrostructure for the fuel stream. Droplets with diameters greater than 40 μm are acceptable under certain combustion conditions. The presence of drops with diameters greater than 100 μm is the main cause of incomplete combustion and pollution of exhaust gases. The drop diameter distribution of droplets is supplemented with an analysis of the percentage distribution of selected diameter classes significant from the point of view of the combustion process in a self-ignition engine.

3.2. Temporal Percentage Distribution of Aerosol Fuel Droplet Diameters in Assumed Size Ranges

A comparison of the time distributions of the fuel droplet diameters belonging to the assumed diameter classes $D_{[1-20]}$, $D_{[20-40]}$, $D_{[40-100]}$, and $D_{[100-1000]}$, obtained as a result of the experiments and constituting the limits of diameters in a given diameter class, is shown in Figures 15–18.

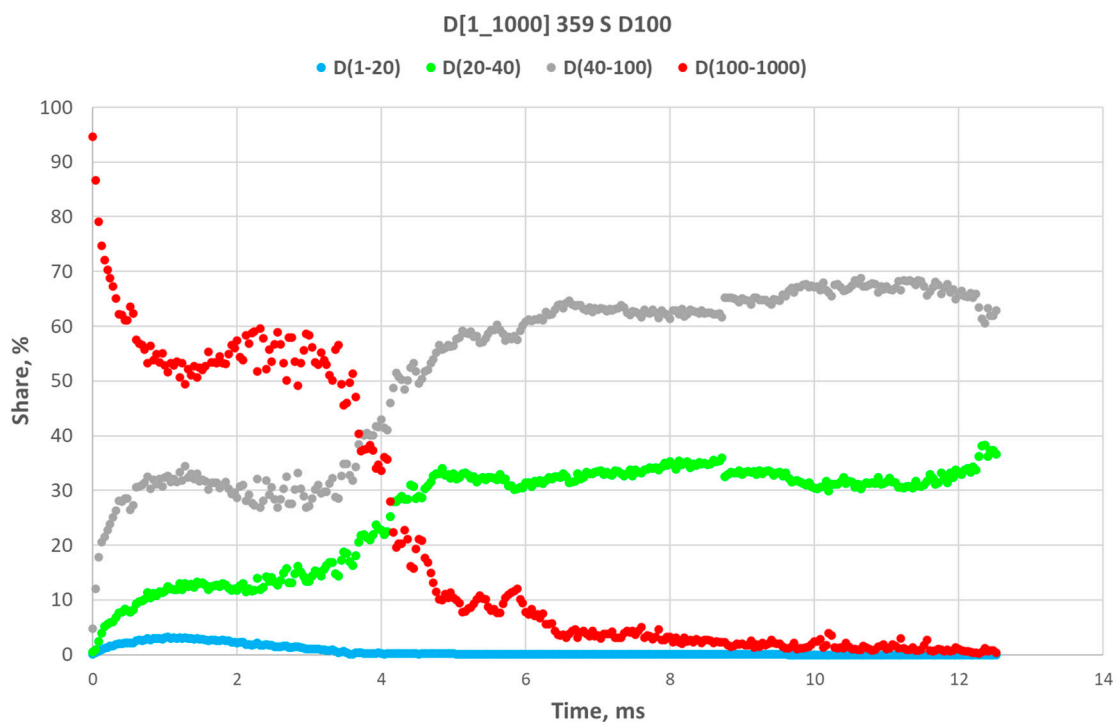


Figure 15. Time drop diameter distribution of the fuel droplet diameters belonging to the diameter classes $D_{[1-20]}$, $D_{[20-40]}$, $D_{[40-100]}$, and $D_{[100-1000]}$ for an spray obtained using a sprayer with a standard (unmodified) needle.

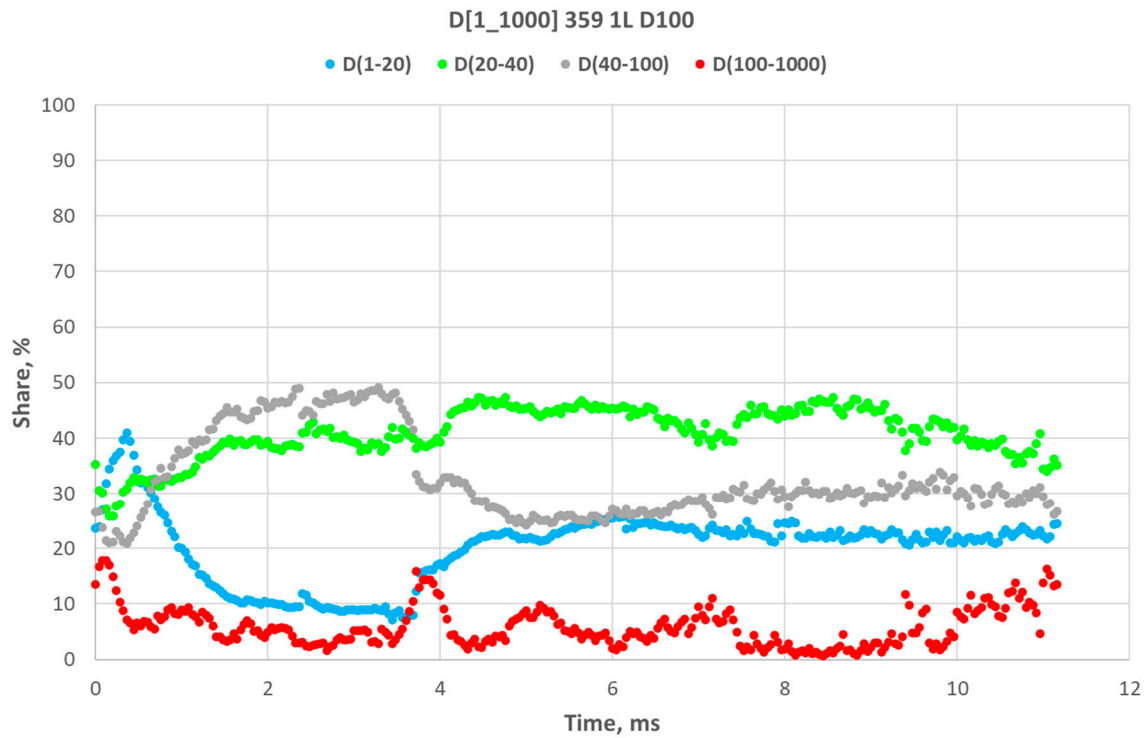


Figure 16. Time drop diameter distribution of the fuel droplet diameters belonging to the diameter classes $D_{[1-20]}$, $D_{[20-40]}$, $D_{[40-100]}$, and $D_{[100-1000]}$ for the spray obtained using a sprayer with a needle profile containing one de Laval nozzle (1L).

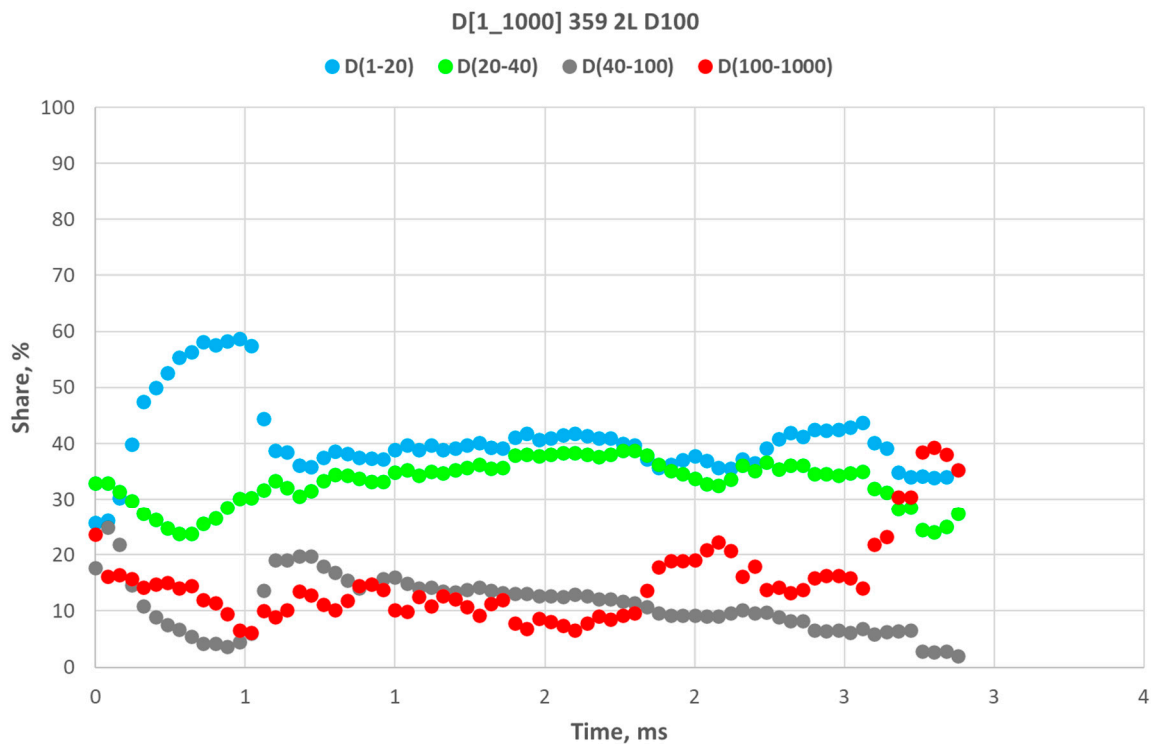


Figure 17. Time drop diameter distribution of the fuel droplet diameters belonging to the diameter classes $D_{[1-20]}$, $D_{[20-40]}$, $D_{[40-100]}$, and $D_{[100-1000]}$ for the spray obtained using a sprayer with a needle and a profile containing two de Laval nozzles (2L).

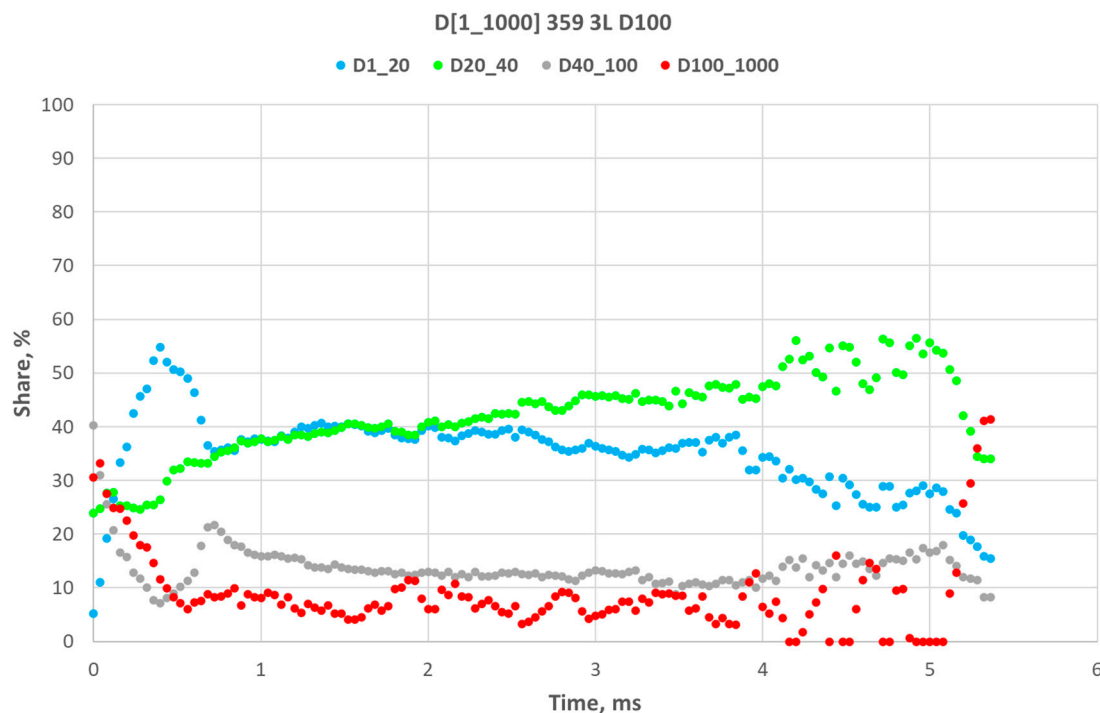


Figure 18. Time drop diameter distribution of the fuel droplet diameters belonging to the diameter classes $D_{[1-20]}$, $D_{[20-40]}$, $D_{[40-100]}$, and $D_{[100-1000]}$ for the spray obtained using a sprayer with a needle profile containing three de Laval nozzles (3L).

The results of the experiment indicate significant differences in the time distribution of arbitrarily selected diameter classes of the fuel spray. In the spray produced by a standard atomizer, after a time interval of about 4 ms needed for the development of the stream, the diameters in the range of 20–40 μm (optimal for the combustion process) had a volume fraction half that of diameters in the range of 40–100 μm , which is potentially problematic in certain combustion conditions.

In the spray produced by modified atomizers, the share of diameters in the optimal range definitely exceeds the share of the other three diameter classes. This confirms the observations resulting from the general drop diameter distribution presented in Figures 15–17. The observation of a higher diameter range for the second modal value, in relation to the modified nozzle with the 2L needle, is also confirmed (Figure 15), and the 3L needle (Figure 18) is compared to the standard nozzle (Figure 15).

The standard atomizer is characterized by a relatively wide range of the percentage of the optimal class of spray diameters of 20–40 μm compared to the modified atomizers. During the entire injection event, it was in the 0.43–38.25% range. The variations in the ranges of the same diameter class for the modified nozzle needles were 25.83–47.39% for the 1L needle, 23.73–38.79% for the 2L needle, and 23.89–56.51% for the 3L needle. Therefore, they were definitely higher and subject to less fluctuation during the injection. The measure of fluctuations is the coefficient of variation in the time distribution of the optimal class of diameters. The standard atomizer is characterized by a high coefficient of variation in the instantaneous share of the 20–40 μm class, equal to 36.66%. This is more than three times higher than the same coefficients for the 1L and 2L needles, which are 11.15% and 12.45%, respectively. Simultaneously, it is twice as high as the 3L needle, which shows the variability of the same class of diameters at 18.30%. At the same time, the 2L needle showed the lowest standard deviation and the lowest average dispersion value for the optimal diameter class for the entire measurement.

Considering the bimodal nature of the drop diameter distribution of the diameters and the minimum percentage share among them corresponding to a diameter of about 150 μm , an analysis of the relationship of two arbitrarily selected diameter classes corresponding to

the ranges of 5–150 μm and 150–1000 μm was performed. The boundaries of these intervals correspond to the groups of the spray characteristic of the core and the remaining part of the stream visible in the drop diameter distribution. Comparison of the time distributions of the quotient of the percentage share of the two groups of diameters, significant from the point of view of the penetration range of the fuel stream, as well as the ignition delay and combustion time, allows for a substantial difference between the standard nozzle and its modifications. The standard nozzle's characteristics strictly depend on the stream's development time. They were subject to significant changes from 3.73 at the start of the measurement through the minimum in the time interval of 1–2 ms and the maximum in the vicinity of 3 ms. The other characteristics show no clear dependence on the jet's development time, despite definitely lower absolute values of fluctuations.

The characteristics of the nozzles with 2L and 3L needles (Figures 17 and 18) show a relatively high level of variability for the considered relationship of the share of diameters at the end of the observation compared to the characteristics of the nozzle with the 1L needle and the standard nozzle (Figures 15 and 16). The evaluated relationship shows the share of droplets with the largest diameters in the range of 150–1000 μm , which is problematic from the point of view of ignition delay and combustion time. The lowest average value of the share of drops with the largest diameters, equal to 4%, is shown by the 1L sprayer. For the remaining solutions, the share of droplets in this range of diameters is in the following order: 9% for the 3L design, 29% for the 2L needle, and 43% for the standard nozzle. All modified nozzles produced spray with a lower content of large-diameter droplets compared to the standard solution.

The analysis of the actual volumetric distribution of the diameters was supplemented in the next stage with a time analysis of the distribution of the derivative parameter in the form of the diameter $D_{[3,2]}$, characterizing the droplet range, and the heat and mass exchange that have a close relationship with ignition delay and combustion quality. In the analysis of fuel combustion processes, the diameter $D_{[3,2]}$ is used to describe the spray macrostructure.

3.3. Temporal Distribution of the Sauter Mean Diameter of Spray Fuel Droplets

A comparison of the time distributions of the Sauter diameter, $D_{[3,2]}$, obtained as a result of the experiments for the atomizer with the tested types of needles, is shown in Figures 19–22. The results of the atomization quality, based on the time analysis of the Sauter mean diameter, $D_{[3,2]}$, indicate that the use of each type of modernization improved the degree of atomization compared to the standard nozzle. This applies to both the average and extreme values. The Sauter mean diameter for the entire spraying period for the sprayer with a standard needle (Figure 19) was 55.3 μm , compared to 26.27 μm for the nozzle with the 1L needle (Figure 20), 18.3 μm for the atomizer with the 2L needle (Figure 21), and 21.2 μm for the nozzle with the 3L needle (Figure 22). The maximum values of $D_{[3,2]}$ observed just after the start of the measurements were 186.7 μm for the standard nozzle compared to 41.3 μm for the 1L needle, 25.5 μm for the 2L needle, and 50.6 μm for the 3L needle. The statistical data on the distribution of $D_{[3,2]}$ indicate that the 2L needle was characterized by the most stable degree of atomization. With the relatively smallest standard deviation of the droplet diameters equal to 2.17 μm and the abovementioned $D_{[3,2]}$ value. A percentage of 66% for the $D_{[3,2]}$ value using the nozzle with the 2L needle is in the range of 16.1–20.5 μm , compared to the range of 38.5–72.0 μm for the standard nozzle, the range of 20.0–32.6 μm for the 1L needle, and 17.1–25.4 μm for the nozzle with the 3L needle.

The degree of atomization resulting from the assessment of the actual distribution of droplet diameters and the Sauter mean diameter, $D_{[3,2]}$, is only one of the two crucial parameters of atomization quality. A precise assessment of the homogeneity of the actual spray volumetric distribution is obtained by analyzing the time distribution of the percentile diameters D_v (10), D_v (50), and D_v (90), as presented below.

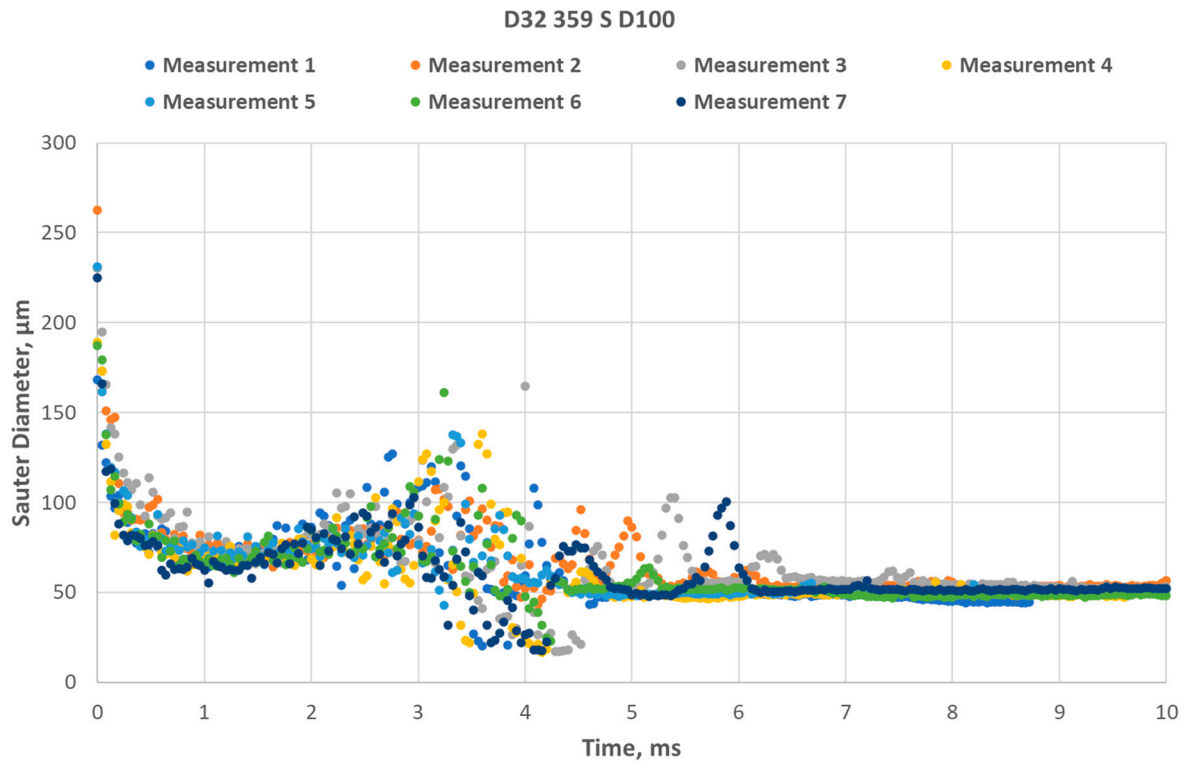


Figure 19. Time distribution of the Sauter mean diameters, $D_{[3,2]}$, of the fuel droplets for the spray obtained using an atomizer with a standard (i.e., unmodified) nozzle needle.

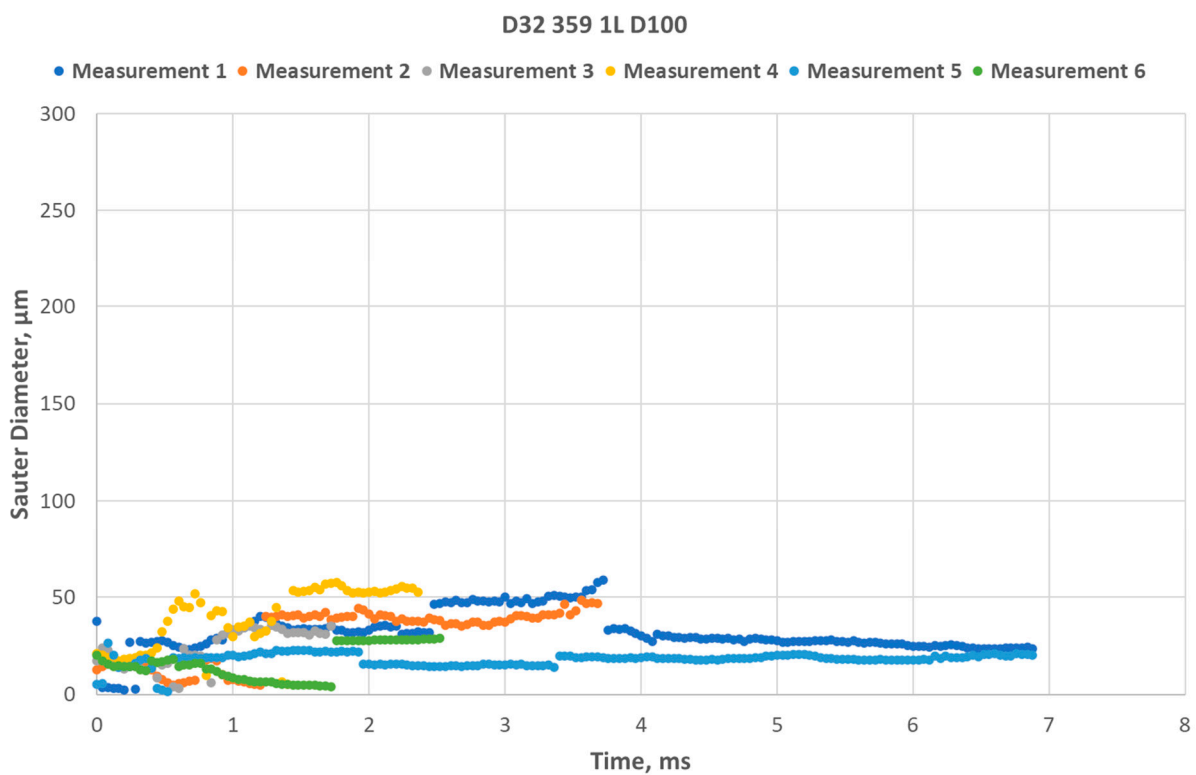


Figure 20. Time distribution of the Sauter mean diameters, $D_{[3,2]}$, of the fuel droplets for the spray obtained using a sprayer with a needle profile containing one de Laval nozzle (1L).

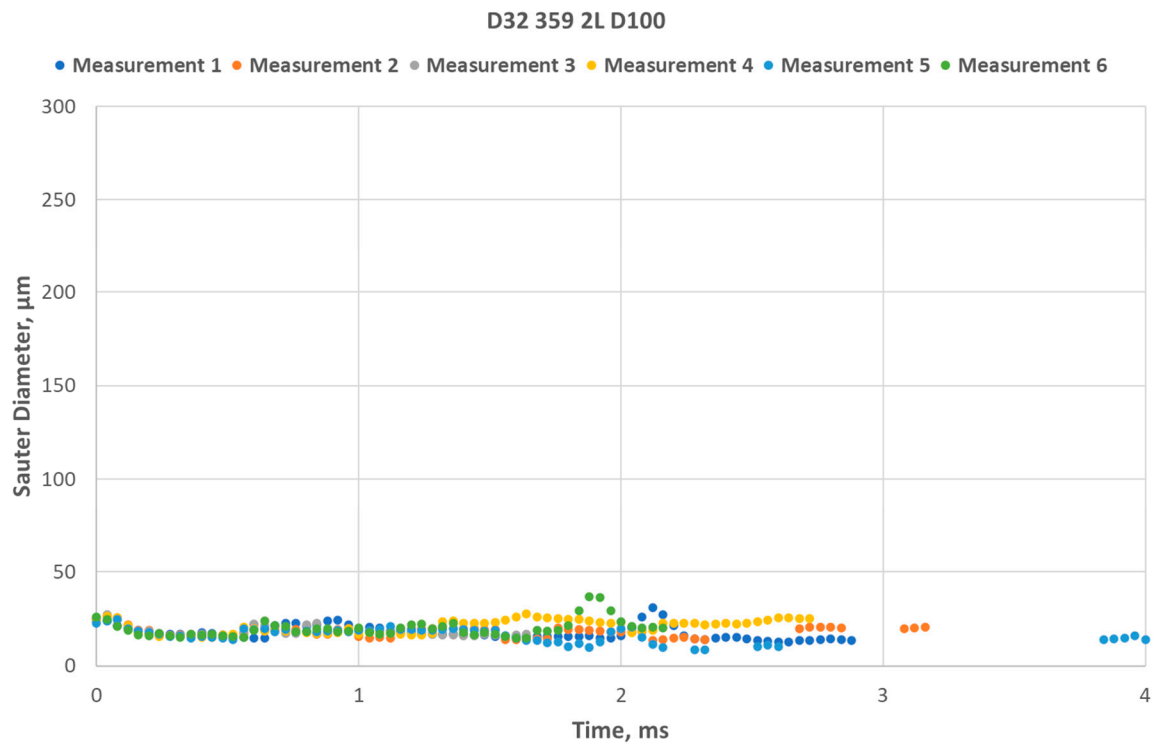


Figure 21. Time distribution of the Sauter mean diameters, $D_{[3,2]}$, of the fuel droplets for the spray obtained using a sprayer with a needle profile containing two de Laval nozzles (2L).

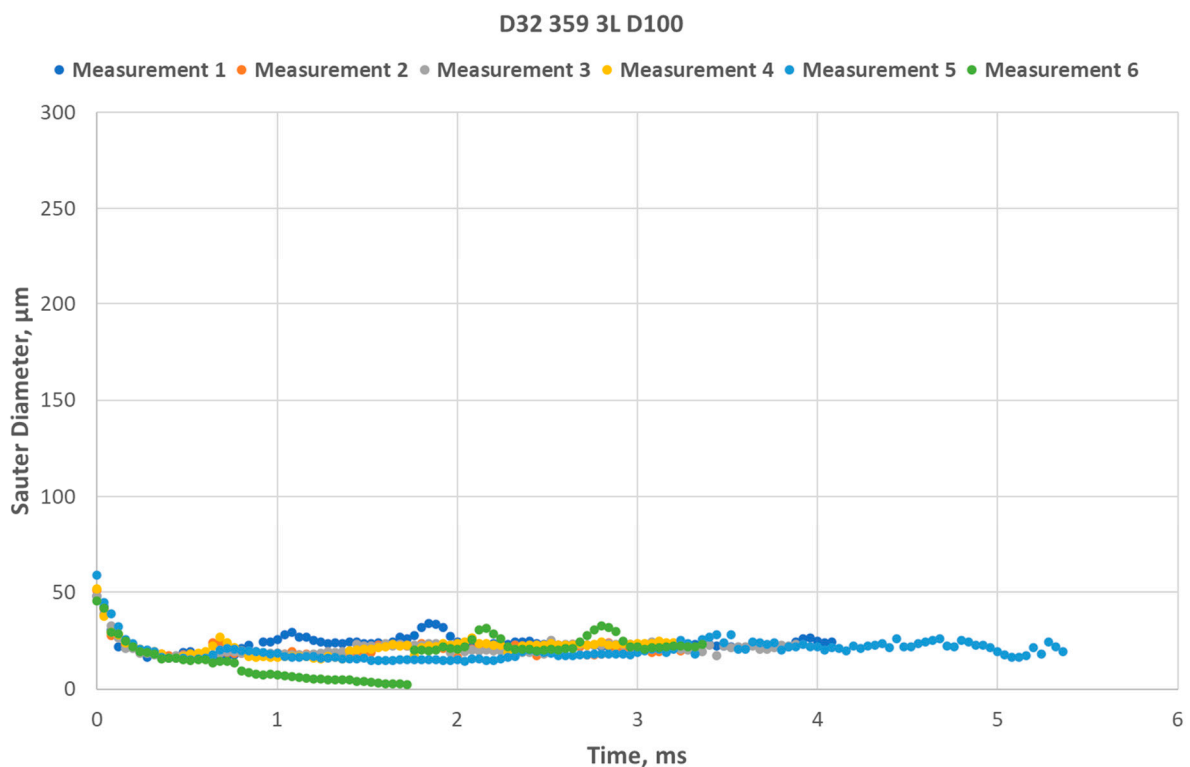


Figure 22. Time distribution of the Sauter mean diameters, $D_{[3,2]}$, of the fuel droplets for the spray obtained using a sprayer with a needle profile containing three de Laval nozzles (3L).

A comparison of the time distributions of the percentiles of the distribution of the droplet diameters D_v (10), D_v (50), and D_v (90), significant from the point of view of

atomization homogeneity and obtained as a result of the experiments using a standard nozzle and its modifications, is shown in Figure 23.

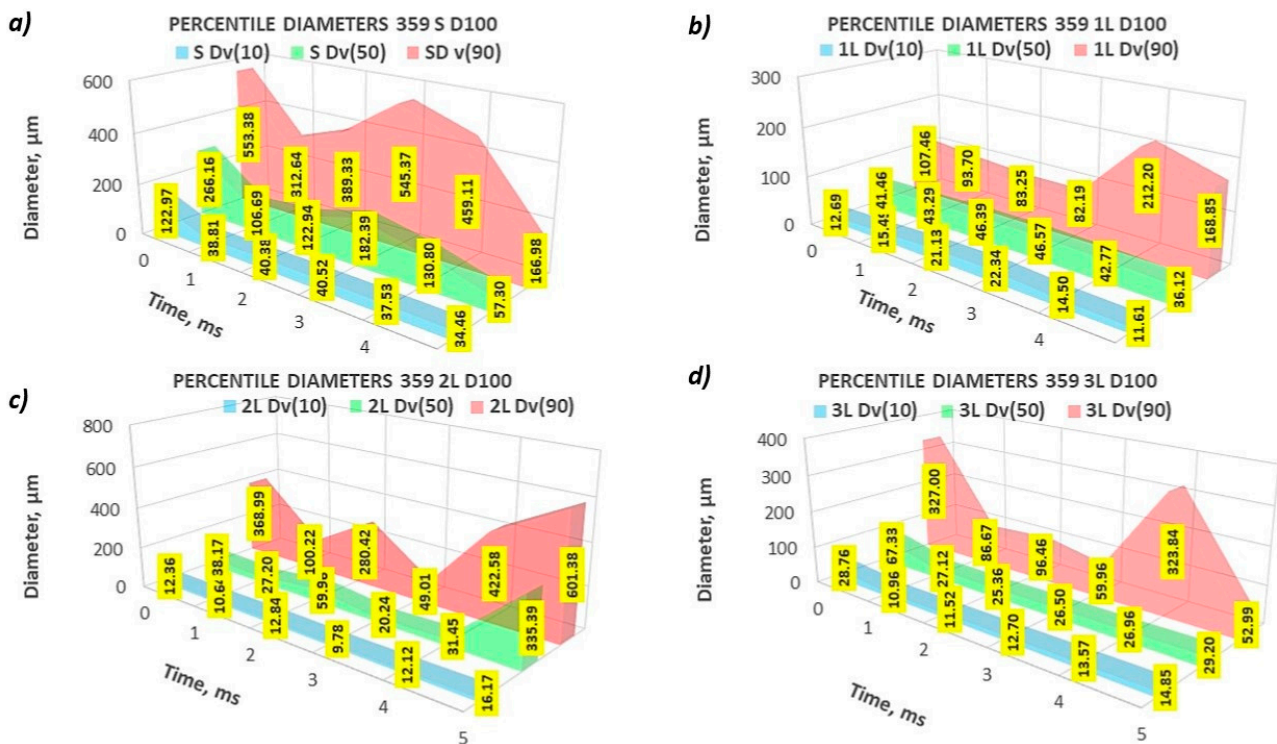


Figure 23. Percentiles of the fuel droplet diameter distribution during spraying using nozzles with tested needles in successive 1 ms spraying time intervals: (a) with a standard needle; with a needle profile containing (b) one de Laval nozzle, (c) two de Laval nozzles, and (d) three de Laval nozzles.

The results presented in Figure 23 indicate the existence of a significant difference in the quality of the spray produced by the atomizer with the standard needle and with the modified versions of the nozzle needle. A standard atomizer's characteristics strictly depend on the time interval of the stream's development. They are subject to significant changes similar to the previously presented time distributions of selected diameter classes.

The values of the percentile diameters were high at the start of the measurement; they reached a minimum in the time interval of 1–2 ms and then a maximum in the interval of 3–4 ms. The characteristics of the modified nozzle needles showed no clear dependence of the percentile diameter values on the stream development time interval, despite definitely lower absolute fluctuation values. The characteristics of the 2L and 3L needles showed a relatively high level of variability in the distribution of the percentile diameters during the entire observation period compared to the characteristics of the 1L and standard needles. This confirms the results presented earlier in this paper in Figures 15–18.

The comparison of the relative widths of the time distributions of the *SPAN* spray droplet diameters obtained during the experiment is shown in Figures 24–27. The span of the diameter distribution is the basic measure of the atomization uniformity. The results of the statistical analysis of the time distribution of the *SPAN* percentile diameters indicate that the application of the modernization improved the homogeneity of the atomization for the variant 1L (Figure 25) compared to the standard nozzle needle (Figure 24). The other modifications (i.e., 2L (Figure 26) and 3L (Figure 27)) showed a greater range of the distribution of the percentile diameters. This applies to both average and extreme values. The average spread value for the standard nozzle needle is 1.89, compared to 2.02 for the 1L needle, 5.21 for the 2L needle, and 4.48 for the 3L needle.

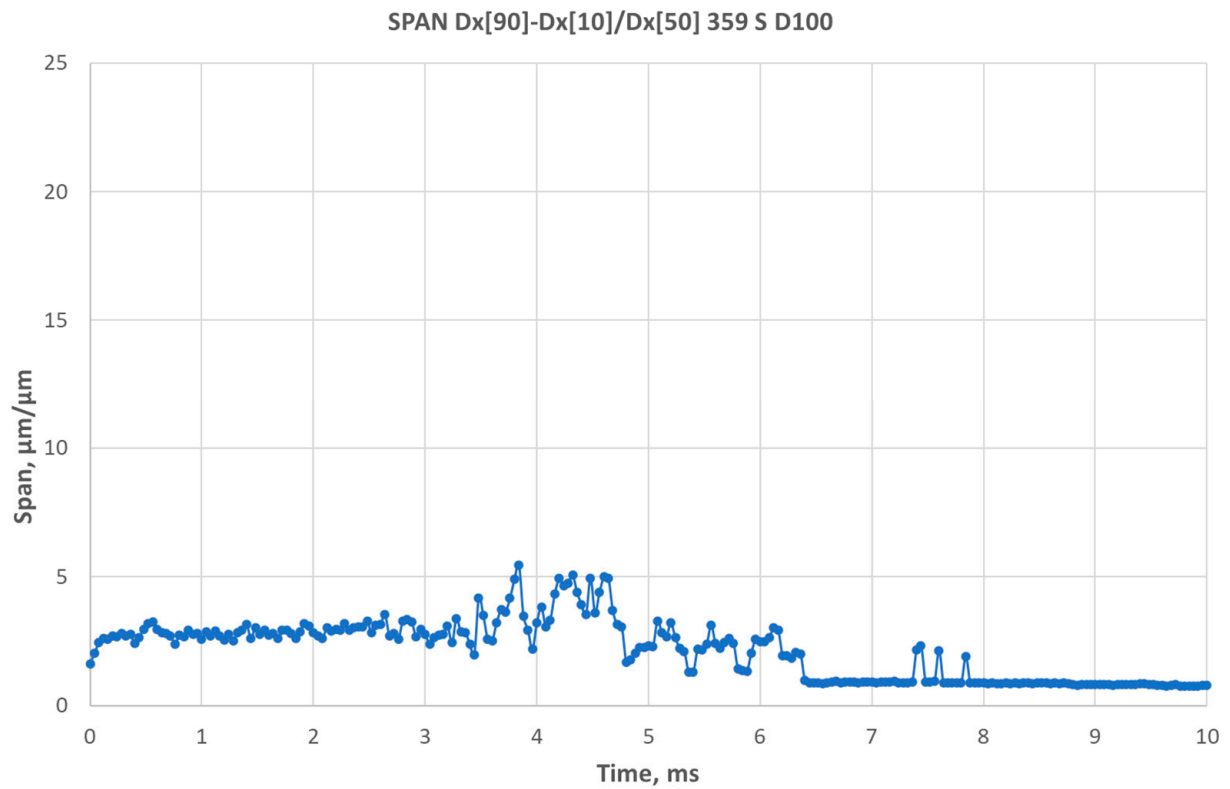


Figure 24. Span of the statistical distribution of the droplet sizes during the fuel atomization process using a nozzle with a standard (i.e., unmodified) needle.

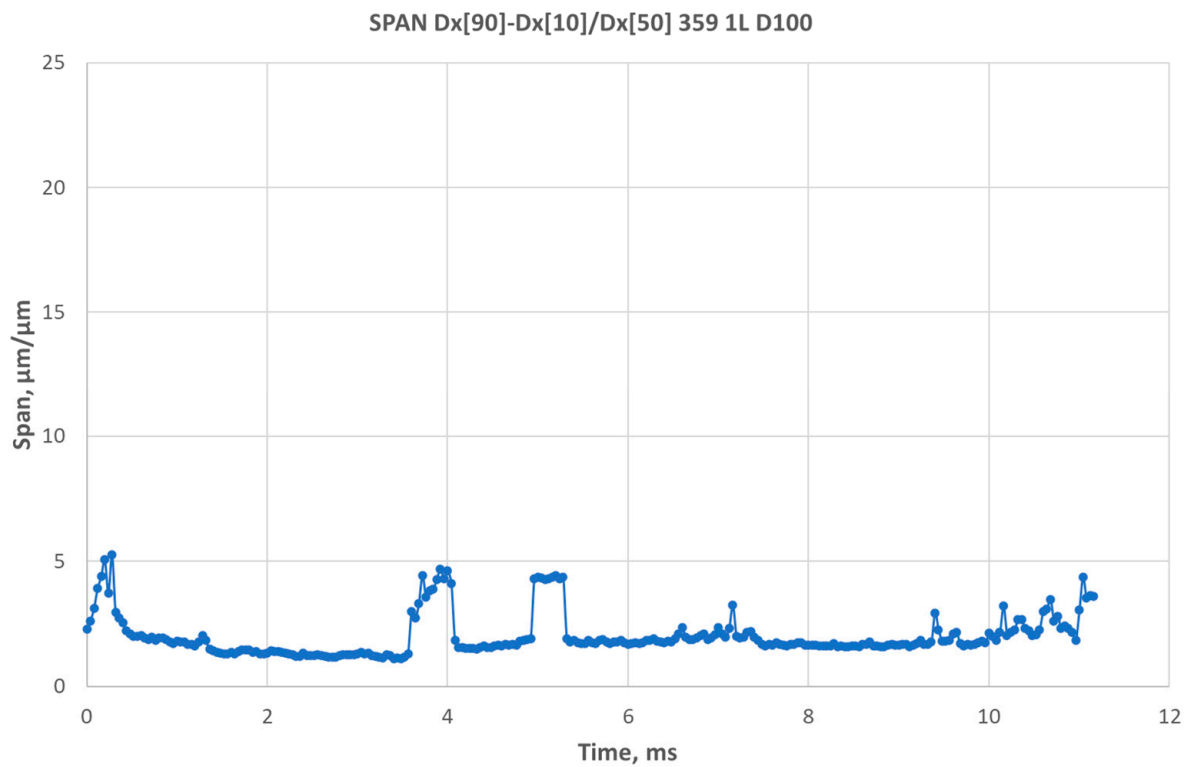


Figure 25. Span of the statistical distribution of the droplet sizes during the fuel atomization process using a nozzle with a needle profile containing one de Laval nozzle (1L).

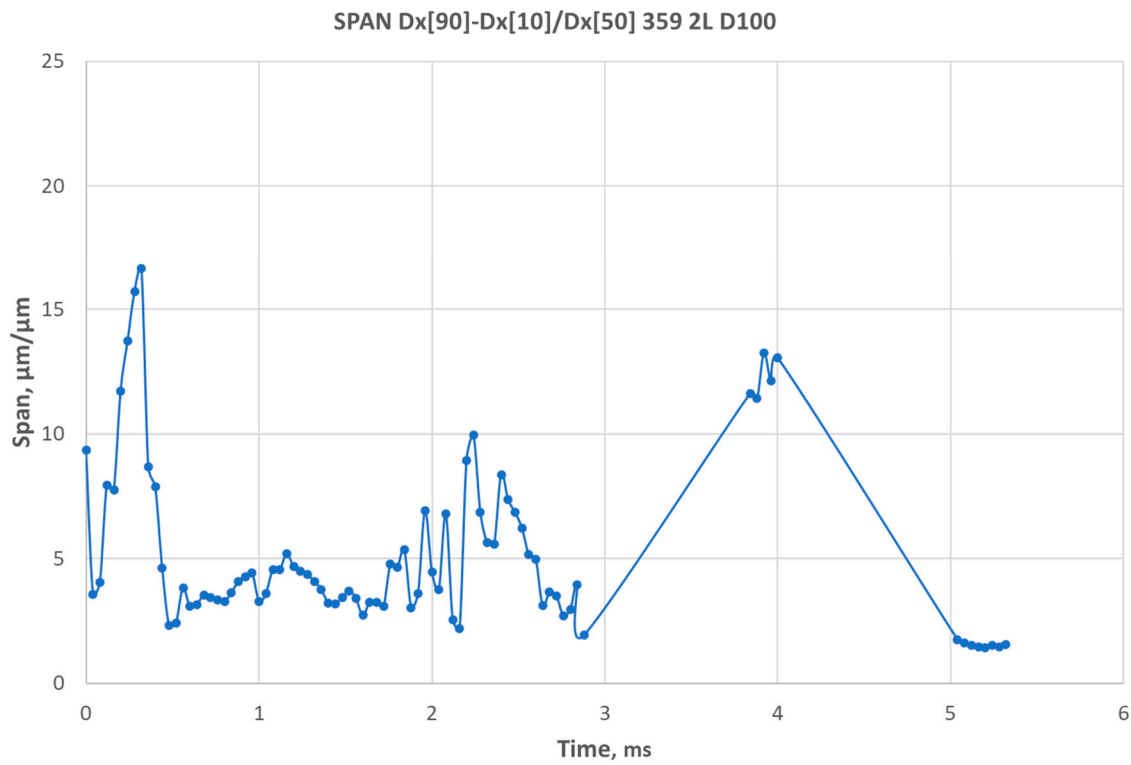


Figure 26. Span of the statistical distribution of the droplet sizes during the fuel atomization process using a nozzle with a needle profile containing two de Laval nozzles (2L).

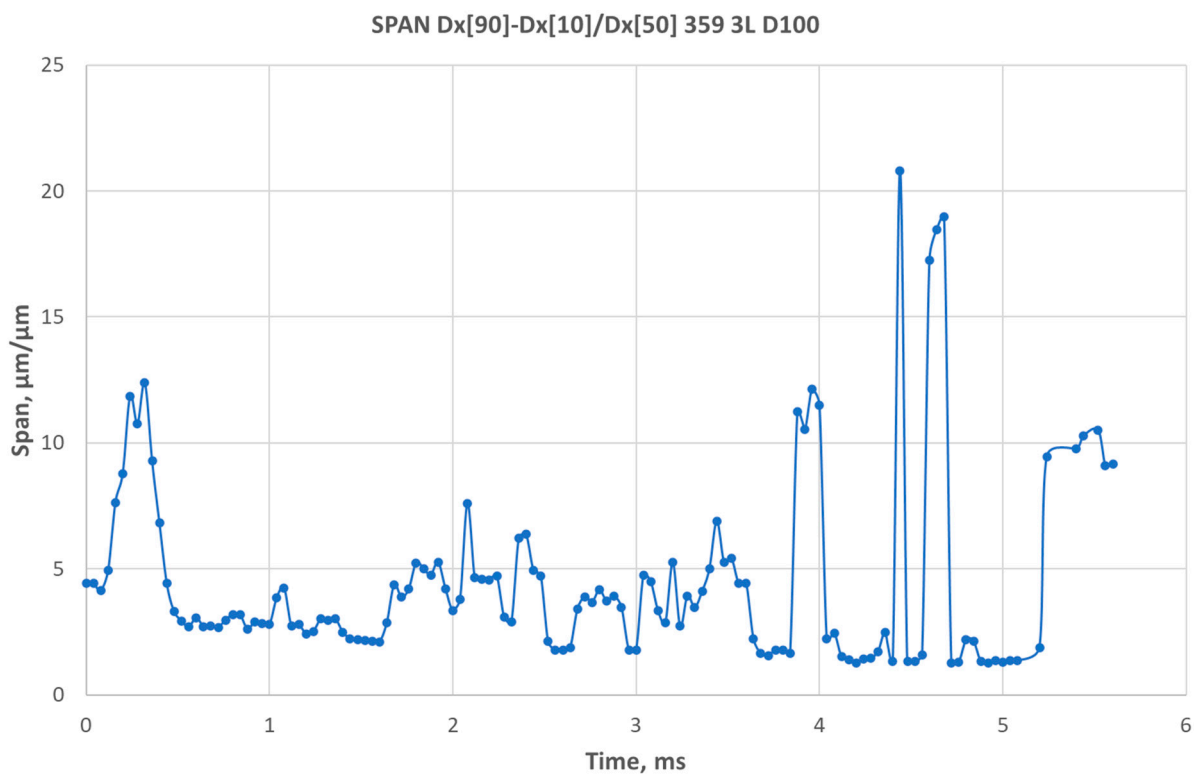


Figure 27. Span of the statistical distribution of the droplet sizes during the fuel atomization process using a nozzle with a needle profile containing three de Laval nozzles (3L).

4. Conclusions

The presented studies broaden the knowledge of the impact of the shape of the flow channel of the sprayer of the tested type, determined by modifying the passive part of the needle, on the key parameters of the drop diameter distribution of the fuel spray produced by the injector during injection into the medium under atmospheric pressure.

The research led to the following conclusions:

- The results of the measurement of the drop diameter distribution imply that the use of nozzles with a modification to the flow channel allows for increasing the share of drops with smaller diameters compared to the standard nozzle. This is due to the greater degree of atomization, which is one of the two conditions for improving the atomization quality. Shifting the distribution of the droplet diameters toward smaller values is important from the point of view of the fuel injection and combustion process in a compression–ignition engine.
- The results of the atomization quality, based on the time analysis of the Sauter mean diameter, $D_{[3,2]}$, indicate that the use of each type of modernization improved the degree of atomization compared to the standard nozzle. This applies to both average and extreme values. Statistical data on the distribution of $D_{[3,2]}$ make it possible to conclude that the 2L atomizer was characterized by the most stable degree of atomization.
- The results of the atomization quality based on the time analysis of the distribution of the percentile diameters $D_v(10)$, $D_v(50)$, and $D_v(90)$ show an improvement in the atomization uniformity of the 1L needle compared to the standard nozzle needle. The remaining modifications, 2L and 3L, displayed a greater range of the distribution of the percentile diameters compared to the standard nozzle. This applies to both average and extreme values.
- The results of the experiment signify significant differences in the time distribution of selected classes of fuel spray diameters. In the spray produced by the standard atomizer, diameters in the range of 20–40 μm (appropriate for proper combustion) had a volume fraction half that of the diameters in the range of 40–100 μm (which is potentially problematic under certain combustion conditions). In the spray produced by all of the modified atomizers, the share of diameters in the optimal range definitely exceeded the share of the other diameter classes.
- The comparison of the time distributions of the relationship of two diameter ranges, resulting from a bimodal distribution, with a limit value of 150 μm (significant from the point of view of the jet penetration range) for the ignition delay and combustion time, allowed for identifying a significant difference between the standard nozzle and its modifications. The characteristics of the spray produced by the standard atomizer strictly depended on the time interval of the stream's development. The characteristics of the 2L and 3L needles showed a relatively higher level of variability in the diameter relationships resulting from the bimodal distribution compared to those of the 1L and standard nozzle needles. The lowest value for the diameter relationship resulting from the bimodality of the distribution was shown by the 1L needle.

The research results presented in the article provide new theoretical knowledge regarding the influence of the shape of the atomizer needle on the characteristics of the generated spray. From an application perspective, this may be used in optimizing the design of injectors to improve the quality of the combustion process. It can, therefore, be used as one of the tools to improve the overall engine efficiency (reducing fuel consumption and reducing CO₂ emission) and/or modify the combustion peak temperature in the cylinder (reducing NO_x emissions).

However, obtaining the abovementioned benefits requires further research into the impact of modifying the needle's shape on the durability of the nozzle due to erosion and cavitation processes inside the nozzle, which may shorten the intervals between replacing injectors in the engine. This requires further R&D work on various types of modifications to injector needles and their impact on the quality of fuel atomization, as well as independently conducted tests of the wear of these needles.

An additional application resulting from the conducted research is the proposed testing approach presented in the publication, which can be used as a method of verifying the relationship between the shape of the passive part of needles and the characteristics of the sprayed fuel.

Author Contributions: Conceptualization, O.K., G.K. and L.C.; methodology, O.K., M.S., G.K. and L.C.; software, O.K., M.S., G.K., P.K. and L.C.; validation, O.K., G.K. and L.C.; formal analysis, L.C., G.K. and L.C.; investigation, O.K., M.S., G.K., P.K., S.O. and L.C.; resources, O.K., M.S., G.K., P.K., S.O. and L.C.; data curation, G.K. and M.S.; writing—original draft preparation, O.K., M.S., G.K., P.K., S.O. and L.C.; writing—review and editing, O.K., M.S., G.K., P.K., S.O. and L.C.; visualization, O.K., M.S., G.K., P.K., S.O. and L.C.; supervision, O.K. and L.C.; project administration, O.K. and L.C.; funding acquisition, O.K. and L.C. All authors have read and agreed to the published version of the manuscript.

Funding: This research outcome was achieved under the research project number 00004-6520.13-OR1600001/19/20, “Reducing energy consumption in terms of reducing the negative impact of inland and sea fishing on the environment”, financed from a subsidy of the EU. This research was also funded by the Ministry of Science and Higher Education (MEiN) of Poland, grant number 1/S/KPBMiM/23.

Data Availability Statement: All data are available in this paper and the dataset: Klyus O., Szczepanek M., Kidacki G., Krause P., Olszowski S., Chybowski L., Effect of needle profile in the ICE fuel injector nozzle on the quality of fuel atomization. Mendeley Data, V1, DOI: [10.17632/ppbt9cztg5.1](https://doi.org/10.17632/ppbt9cztg5.1), <https://data.mendeley.com/datasets/ppbt9cztg5/1> [75].

Acknowledgments: Laboratory tests were performed on behalf of the authors at the Center for Testing Fuels, Working Fluids, and Environmental Protection (CBPCrIOS) of the Maritime University of Szczecin.

Conflicts of Interest: The authors declare no conflicts of interest.

Abbreviations and Symbols

3D	three dimensions
1L, 2L, 3L	designations of the profiles of the passive part of the atomizer needle
A	area at the nozzle exit
A_p	external particle surface area
C_D	discharge coefficient
CN	cetane number
CO ₂	carbon dioxide
D100	diesel oil without biocomponents
D	particle diameter
$D_{[2,0]}$	surface diameter
$D_{[3,0]}$	volume diameter
$D_{[3,2]}$	Sauter diameter
$D_{[p,q]}$	particle diameter in moment-ratio notation
$D_{[x_1-x_2]}$	class of droplet diameters covering all drops with diameters in the range $[x_1, x_2]$
D_v	percentile of the volume distribution of droplet size (diameter)
d_N	atomizer slot diameter
i	number of the size class with upper particle size x_i
ISO	International Organization for Standardization
K	cavitation number
L	channel length atomizer
\dot{m}	fuel mass flow
n	number of particles in the i -th size class
N	number of size classes
NIST	National Institute of Standards and Technology
NO _x	general designation of NO and NO ₂ nitrogen oxides

Oh	Ohnesorge number
Δp_w	differential pressure
p_{air}	air pressure in space
p_{inj}	injection pressure
Re	Reynolds number
R&D	research and development
SMD	Sauter mean diameter
SPAN	relative width of the statistical distribution of droplet sizes in the mixture volume
V_p	particle volume
We	Weber number
w	fuel flow rate from the nozzle
x_1, x_2	limits of the range defining a given class of fuel droplet diameters
φ	discharge coefficient, including losses related to the shape of the atomizer nozzle channel
μ	fuel dynamic viscosity
ν	kinematic viscosity of the fuel
ρ	density of the fuel
σ	surface tension cohesive forces of fuel

References

- Ranganathan, S.; Kumar, S.; Thirunavukkarasu, S.; Muthuswamy, S.P. *Modular Design and Analyze of Air Intake Manifold for Formula Vehicle*; SAE International: Warrendale, PA, USA, 2020.
- Yerrennagoudaru, H.; Desai, S. Effect of inlet air swirl on four stroke single cylinder diesel engine's performance. *IOSR J. Mech. Civ. Eng.* **2014**, *11*, 59–68. [[CrossRef](#)]
- Luo, W.; Liu, H.; Liu, L.; Liu, D.; Wang, H.; Yao, M. Effects of scavenging port angle and combustion chamber geometry on combustion and emission of a high-pressure direct-injection natural gas marine engine. *Int. J. Green Energy* **2023**, *20*, 616–628. [[CrossRef](#)]
- Harshavardhan, B.; Mallikarjuna, J.M. *Effect of Combustion Chamber Shape on In-Cylinder Flow and Air-Fuel Interaction in a Direct Injection Spark Ignition Engine—A CFD Analysis*; SAE International: Warrendale, PA, USA, 2015.
- Pakale, P.N. Review on Cylinder Head Design for Swirl Optimization. *Int. J. Eng. Res.* **2020**, *9*. [[CrossRef](#)]
- Klyus, O.; Zamiatina, N. Residual fuel atomization process simulation. *Combust. Engines* **2017**, *169*, 108–112. [[CrossRef](#)]
- Chybowski, L.; Szczepanek, M.; Gawdzińska, K.; Klyus, O. Particles Morphology of Mechanically Generated Oil Mist Mixtures of SAE 40 Grade Lubricating Oil with Diesel Oil in the Context of Explosion Risk in the Crankcase of a Marine Engine. *Energies* **2023**, *16*, 3915. [[CrossRef](#)]
- Yang, L.; Fu, Q.; Zhang, W.; Du, M.; Tong, M. Atomization of gelled propellants from swirl injectors with leaf spring in swirl chamber. *At. Sprays* **2011**, *21*, 949–969. [[CrossRef](#)]
- Zhang, Z.; Liu, H.; Yue, Z.; Wu, Y.; Kong, X.; Zheng, Z.; Yao, M. Effects of Multiple Injection Strategies on Heavy-Duty Diesel Energy Distributions and Emissions Under High Peak Combustion Pressures. *Front. Energy Res.* **2022**, *10*, 857077. [[CrossRef](#)]
- Nozdrzykowski, K. Force analysis and simulation—Experimental research on the measurement of cylindrical surface. *Zesz. Nauk. Akad. Morskiej Szczecinie Sci. J. Marit. Univ. Szczec.* **2016**, *48*, 37–42.
- Włodarski, J.; Podsiadło, A.; Kluj, S. *Uszkodzenia Systemu Tłok-Cylinder (TC) Okrętowych Silników Spalinowych*; Wydawnictwo Akademii Morskiej w Gdyni: Gdynia, Poland, 2011.
- Borkowski, T.; Kowalak, P.; Myśków, J. Vessel main propulsion engine performance evaluation. *J. KONES* **2012**, *19*, 53–60. [[CrossRef](#)]
- Kowalak, P.; Borkowski, T.; Bonisławski, M.; Hołub, M.; Myśków, J. A statistical approach to zero adjustment in torque measurement of ship propulsion shafts. *Measurement* **2020**, *164*, 108088. [[CrossRef](#)]
- Zhang, Z.; Liu, H.; Yue, Z.; Li, Y.; Liang, H.; Kong, X.; Zheng, Z.; Yao, M. Effects of intake high-pressure compressed air on thermal-work conversion in a stationary diesel engine. *Int. J. Green Energy* **2023**, *20*, 338–351. [[CrossRef](#)]
- Bogdanowicz, A.; Kniaziewicz, T. Marine Diesel Engine Exhaust Emissions Measured in Ship's Dynamic Operating Conditions. *Sensors* **2020**, *20*, 6589. [[CrossRef](#)] [[PubMed](#)]
- ASTM D6890-22; Standard Test Method for Determination of Ignition Delay and Derived Cetane Number (DCN) of Diesel Fuel Oils by Combustion in a Constant Volume Chamber. ASTM: West Conshohocken, PA, USA, 2022.
- ASTM D4737-21; Standard Test Method for Calculated Cetane Index by Four Variable Equation. ASTM: West Conshohocken, PA, USA, 2021.
- ASTM D 7668-17; Standard Test Method for Determination of Derived Cetane Number (DCN) of Diesel Fuel Oils Ignition Delay and Combustion Delay Using a Constant Volume Combustion Chamber Method. ASTM: West Conshohocken, PA, USA, 2017.
- Ramadan, O.; Menard, L.; Gardiner, D.; Wilcox, A.; Webster, G. *Performance Evaluation of the Ignition Quality Testers Equipped with TALM Precision Package (TALM-IQTTM) Participating in the ASTM NEG Cetane Number Fuel Exchange Program*; SAE Technical Paper; SAE International: Warrendale, PA, USA, 2017. [[CrossRef](#)]

20. Burgoyne, J.; Cohen, L. The effect of drop size on flame propagation in liquid aerosols. *Proc. R. Soc. Lond. Ser. A Math. Phys. Sci.* **1954**, *225*, 375–392. [CrossRef]
21. Wärtsilä Wärtsilä Introduces New Pre-Swirl Stator. Available online: <https://www.wartsila.com/media/news/07-11-2017-wartsila-introduces-an-innovative-pre-swirl-stator-to-improve-fuel-efficiency> (accessed on 21 November 2020).
22. Babrauskas, V. *Ignition Handbook*; Society of Fire Protection Engineers: Gaithersburg, MD, USA, 2003.
23. Heywood, J.B. *Internal Combustion Engine Fundamentals*; McGraw-Hill, Inc.: New York, NY, USA, 1988; ISBN 0-07-028637-X.
24. Bielecki, Z.; Ochowiak, M.; Włodarczak, S.; Krupińska, A.; Matuszak, M.; Lewtak, R.; Dziuba, J.; Szajna, E.; Choiński, D.; Odziomek, M. The Analysis of the Possibility of Feeding a Liquid Catalyst to a Coal Dust Channel. *Energies* **2021**, *14*, 8521. [CrossRef]
25. Włodarski, K.K.; Witkowski, K. *Okrętowe Silniki Spalinowe. Podstawy Teoretyczne*; Akademia Morska w Gdyni: Gdynia, Poland, 2006.
26. Sauter, J. *Untersuchung der von Spritzvergasern Gelieten Zerstäubung, Forschungsarbeiten auf dem Gebiete des Ingenieurwesens*; Heft 312; VDI-Verlag: Berlin, Germany, 1928.
27. Sauter, J. *Die Grössenbestimmung von Brennstoffteilchen, Forschungsarbeiten auf dem Gebiete des Ingenieurwesens (Mitteilung aus dem Laboratorium für Technische Physik der Technischen Hochschule München)*; Heft 279; VDI-Verlag: Berlin, Germany, 1926.
28. Li, T.; Nishida, K.; Hiroyasu, H. Droplet size distribution and evaporation characteristics of fuel spray by a swirl type atomizer. *Fuel* **2011**, *90*, 2367–2376. [CrossRef]
29. Xiong, H.; Sun, W. Investigation of Droplet Atomization and Evaporation in Solution Precursor Plasma Spray Coating. *Coatings* **2017**, *7*, 207. [CrossRef]
30. Sher, E.; Bar-Kohany, T.; Rashkovan, A. Flash-boiling atomization. *Prog. Energy Combust. Sci.* **2008**, *34*, 417–439. [CrossRef]
31. ISO 9276-2; Representation of Results of Particle Size Analysis—Part 2: Calculation of Average Particle Sizes/Diameters and Moments from Particle size Distributions. ISO: Geneva, Switzerland, 2014.
32. Bielecki, Z.; Ochowiak, M.; Włodarczak, S.; Krupińska, A.; Matuszak, M.; Jagiełło, K.; Dziuba, J.; Szajna, E.; Choiński, D.; Odziomek, M.; et al. The Optimal Diameter of the Droplets of a High-Viscosity Liquid Containing Solid State Catalyst Particles. *Energies* **2022**, *15*, 3937. [CrossRef]
33. Malvern Instruments. *Spraytec User Manual*; Malvern Instruments: Worcestershire, UK, 2007.
34. Sun, Z.-Y.; Li, G.-X.; Yu, Y.-S.; Gao, S.-C.; Gao, G.-X. Numerical investigation on transient flow and cavitation characteristic within nozzle during the oil drainage process for a high-pressure common-rail DI diesel engine. *Energy Convers. Manag.* **2015**, *98*, 507–517. [CrossRef]
35. Ommi, F.; Alavioun, S.S.A.; Mirmohammadi, A.; Nekofar, K. Reviewing the Forces on the Drops of Fuel into the Combustion Chamber of Diesel OM-355 with a Numerical Simulation. *Aust. J. Basic Appl. Sci.* **2011**, *5*, 2513–2521.
36. Hyrouki, H.; Toshikazu, K. Fuel droplet size distribution in diesel combustion chamber. *Bull. JSME* **1976**, *19*, 1064–1072.
37. Brun, R. *Szybkobieżne Silniki Wysokopreżene*; WKiŁ: Warszawa, Poland, 1973.
38. Ghurri, A.; Kim, J.-D.; Kim, H.G.; Jung, J.-Y.; Song, K.-K. The effect of injection pressure and fuel viscosity on the spray characteristics of biodiesel blends injected into an atmospheric chamber. *J. Mech. Sci. Technol.* **2012**, *26*, 2941–2947. [CrossRef]
39. Desantes, J.M.; Arrègle, J.; Pastor, J.V.; Delage, A. Influence of the Fuel Characteristics on the Injection Process in a D.I. Diesel Engine. *J. Engines* **1998**, *107*, 1185–1195.
40. Brandão, L.F.P.; Suarez, P.A.Z. Study of kinematic viscosity, volatility and ignition quality properties of butanol/diesel blends. *Braz. J. Chem. Eng.* **2018**, *35*, 1405–1414. [CrossRef]
41. Blaisot, J.B.; Yon, J. Droplet size and morphology characterization for dense sprays by image processing: Application to the Diesel spray. *Exp. Fluids* **2005**, *39*, 977–994. [CrossRef]
42. Chybowski, L. Study of the Relationship between the Level of Lubricating Oil Contamination with Distillation Fuel and the Risk of Explosion in the Crankcase of a Marine Trunk Type Engine. *Energies* **2023**, *16*, 683. [CrossRef]
43. Ships Business Fuel Oil (FO) Injection Viscosity Control for a Marine Diesel Engine. Available online: <http://shipsbusiness.com/fuel-oil-viscosity-control.html> (accessed on 17 May 2023).
44. Szczepanek, M. Biofuels as an alternative fuel for West Pomeranian fishing fleet. *J. Phys. Conf. Ser.* **2019**, *1172*, 012074. [CrossRef]
45. Hiroyasu, H.; Arai, M.; Tabata, M. Empirical Equations for the Sauter Mean Diameter of a Diesel Spray. *J. Engines* **1989**, *98*, 868–877.
46. Ashgriz, N. (Ed.) *Handbook of Atomization and Sprays*; Springer: Boston, MA, USA, 2011; ISBN 978-1-4419-7263-7.
47. Moreau, J.; Simonin, O.; Habchi, C. A Numerical Study of Cavitation Influence on Diesel Jet Atomisation. In Proceedings of the ILASS Europe Conference, Nottingham, UK, 6–8 September 2004; pp. 1–6.
48. McKinley, G.H.; Renardy, M. Wolfgang von Ohnesorge. *Phys. Fluids* **2011**, *23*, 127101. [CrossRef]
49. Turner, M.R.; Sazhin, S.S.; Healey, J.J.; Crua, C.; Martynov, S.B. A breakup model for transient Diesel fuel sprays. *Fuel* **2012**, *97*, 288–305. [CrossRef]
50. Payri, R.; Guardiola, C.; Salvador, F.J.; Gimeno, J. Critical cavitation number determination in diesel injection nozzles. *Exp. Tech.* **2004**, *28*, 49–52. [CrossRef]
51. Abderrezzak, B.; Huang, Y. A contribution to the understanding of cavitation effects on droplet formation through a quantitative observation on breakup of liquid jet. *Int. J. Hydrog. Energy* **2016**, *41*, 15821–15828. [CrossRef]
52. Lefebvre, A.H.; McDonell, V.G. *Atomization and Sprays*, 2nd ed.; CRC Press: Boca Raton, FL, USA, 2017; ISBN 9781315120911.

53. Chybowski, L.; Kowalak, P.; Dąbrowski, P. Assessment of the Impact of Lubricating Oil Contamination by Biodiesel on Trunk Piston Engine Reliability. *Energies* **2023**, *16*, 5056. [[CrossRef](#)]
54. Mohan, B.; Yang, W.; Chou, S. Development of an accurate cavitation coupled spray model for diesel engine simulation. *Energy Convers. Manag.* **2014**, *77*, 269–277. [[CrossRef](#)]
55. Cristofaro, M.; Edelbauer, W.; Koukouvinis, P.; Gavaises, M. A numerical study on the effect of cavitation erosion in a diesel injector. *Appl. Math. Model.* **2020**, *78*, 200–216. [[CrossRef](#)]
56. Orley, F.M. *Numerical Simulation of Cavitating Flows in Diesel Injection Systems*; TU Munchen: Munchen, Germany, 2015.
57. Lee, W.G.; Reitz, R.D. A Numerical Investigation of Transient Flow and Cavitation within Minisac and Valve-Covered Orifice Diesel Injector Nozzles. *J. Eng. Gas Turbines Power* **2010**, *132*, 052802. [[CrossRef](#)]
58. Alam, M.M.A.; Setoguchi, T.; Matsuo, S.; Kim, H.D. Nozzle geometry variations on the discharge coefficient. *Propuls. Power Res.* **2016**, *5*, 22–33. [[CrossRef](#)]
59. Schmidt, D.P.; Rutland, C.J.; Corradini, M.L.; Roosen, P.; Genge, O. Cavitation in Two-Dimensional Asymmetric Nozzles. *J. Engines* **1999**, *108*, 613–629.
60. Dabiri, S.; Sirignano, W.A.; Joseph, D.D. Cavitation in an orifice flow. *Phys. Fluids* **2007**, *19*, 072112. [[CrossRef](#)]
61. Price, R.J.; Blazina, D.; Smith, G.C.; Davies, T.J. Understanding the impact of cavitation on hydrocarbons in the middle distillate range. *Fuel* **2015**, *156*, 30–39. [[CrossRef](#)]
62. Mohan, B.; Yang, W.; Chou, S. Cavitation in Injector Nozzle Holes—A Parametric Study. *Eng. Appl. Comput. Fluid. Mech.* **2014**, *8*, 70–81. [[CrossRef](#)]
63. Park, S.H.; Suh, H.K.; Lee, C.S. Effect of Cavitating Flow on the Flow and Fuel Atomization Characteristics of Biodiesel and Diesel Fuels. *Energy Fuels* **2008**, *22*, 605–613. [[CrossRef](#)]
64. Molina, S.; Salvador, F.J.; Carreres, M.; Jaramillo, D. A computational investigation on the influence of the use of elliptical orifices on the inner nozzle flow and cavitation development in diesel injector nozzles. *Energy Convers. Manag.* **2014**, *79*, 114–127. [[CrossRef](#)]
65. Winklhofer, E.; Kelz, E.; Morozov, A. Basic flow processes in high pressure fuel injection equipment. In Proceedings of the International Conference on Liquid Atomization and Spray Systems, Sorrento, Italy, 13–17 July 2003; pp. 1–13.
66. He, Z.; Zhong, W.; Wang, Q.; Jiang, Z.; Shao, Z. Effect of nozzle geometrical and dynamic factors on cavitating and turbulent flow in a diesel multi-hole injector nozzle. *Int. J. Therm. Sci.* **2013**, *70*, 132–143. [[CrossRef](#)]
67. He, Z.; Tao, X.; Zhong, W.; Leng, X.; Wang, Q.; Zhao, P. Experimental and numerical study of cavitation inception phenomenon in diesel injector nozzles. *Int. Commun. Heat Mass Transf.* **2015**, *65*, 117–124. [[CrossRef](#)]
68. Mitroglou, N.; Stamboliyski, V.; Karathanassis, I.K.; Nikas, K.S.; Gavaises, M. Cloud cavitation vortex shedding inside an injector nozzle. *Exp. Therm. Fluid Sci.* **2017**, *84*, 179–189. [[CrossRef](#)]
69. Sa, B.; Klyus, O.; Markov, V.; Kamaltdinov, V. A numerical study of the effect of spiral counter grooves on a needle on flow turbulence in a diesel injector. *Fuel* **2021**, *290*, 120013. [[CrossRef](#)]
70. Klyus, O.; Mysłowski, J.; Osipowicz, T. Wtryskiwacza. Paliwa. Patent 205428, 28 December 2006.
71. Klyus, O.; Elias, J.; Klyus, I. Wtryskiwacz. Paliwa. Patent 239493, 11 January 2016.
72. WSK PRW3. Próbnik Wtryskiwaczy. Available online: http://www.wsk.com.pl/wtrysk_2.html (accessed on 26 January 2023).
73. Hahn, D.W. Light Scattering Theory. Available online: <http://plaza.ufl.edu/dwhahn/RayleighandMieLightScattering.pdf> (accessed on 26 February 2023).
74. Jenkins, F.A.; White, H.E. *Fundamentals of Optics*; IV; McGraw-Hill Higher Education: Boston, FL, USA, 2001.
75. Klyus, O.; Szczepanek, M.; Kidacki, G.; Krause, P.; Olszowski, S.; Chybowski, L. *Dataset: Effect of Needle Profile in the ICE Fuel Injector Nozzle on the Quality of Fuel Atomisation*; Maritime University of Szczecin: Szczecin, Poland, 2023.

Disclaimer/Publisher’s Note: The statements, opinions and data contained in all publications are solely those of the individual author(s) and contributor(s) and not of MDPI and/or the editor(s). MDPI and/or the editor(s) disclaim responsibility for any injury to people or property resulting from any ideas, methods, instructions or products referred to in the content.